3 DESIGN OF THE EXPERIMENTAL TESTS

The 3-D full-scale tests were performed at the laboratory of Material and Testing of the University of Trento. The facilities of the laboratory were the starting point for planning the 3-D tests. The lab is equipped with a 42 m long strong floor and to the 9.5 m height reaction L shaped wall (Figure 3-1 and Figure 3-2). Holes in a regular pattern on both the floor and the reaction wall allowing an easy connection of specimens and actuators. Two bridge-cranes allow an easy handling of the specimens. A high pressure oil network characterized by 210 bar, 1500 l/min flow in the main line, 1200 l/min flow in the raising line and 600 kW oil pumps allows the effective connection of several actuators, also distributing them in far apart locations. A support for a queen post truss permanently located in the lab and an emergency escape at the end of the lab limited the available area for test to a square area with side of approximately 13.6 m (Figure 3-3).

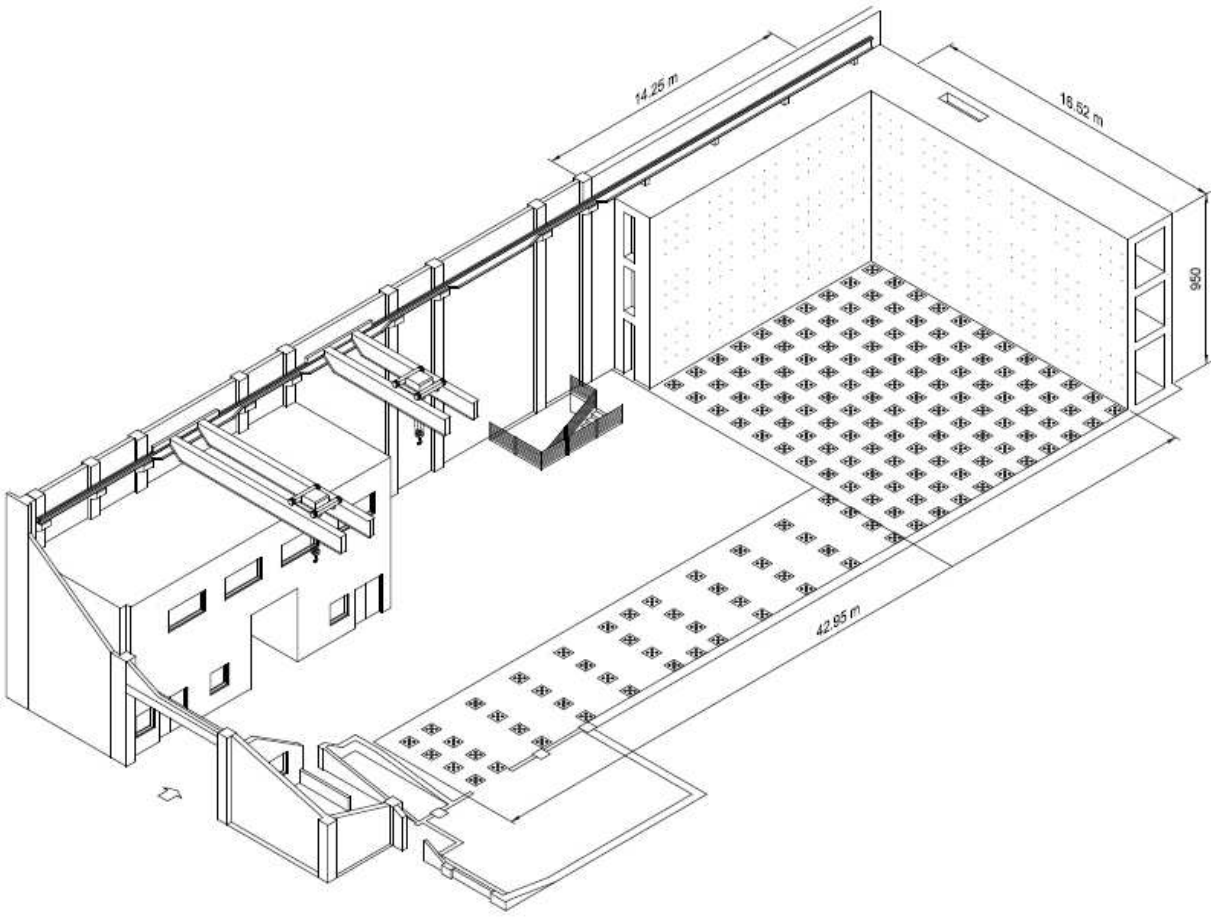

Figure 3-1: 3-D view of the laboratory of Material and Testing of the University of Trento

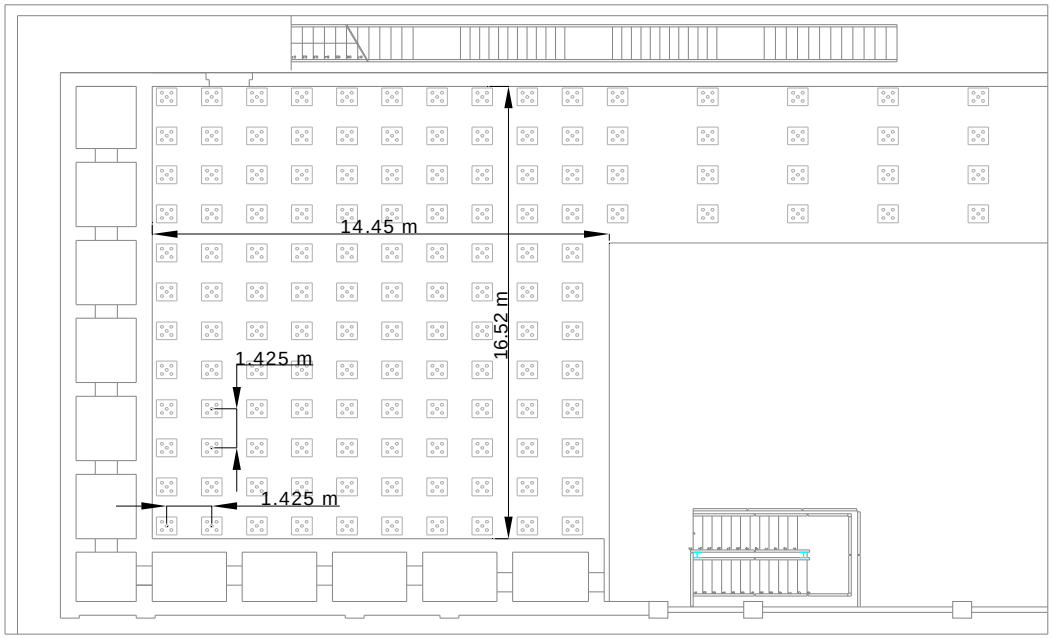

Figure 3-2: Plan view of the laboratory of Material and Testing of the University of Trento

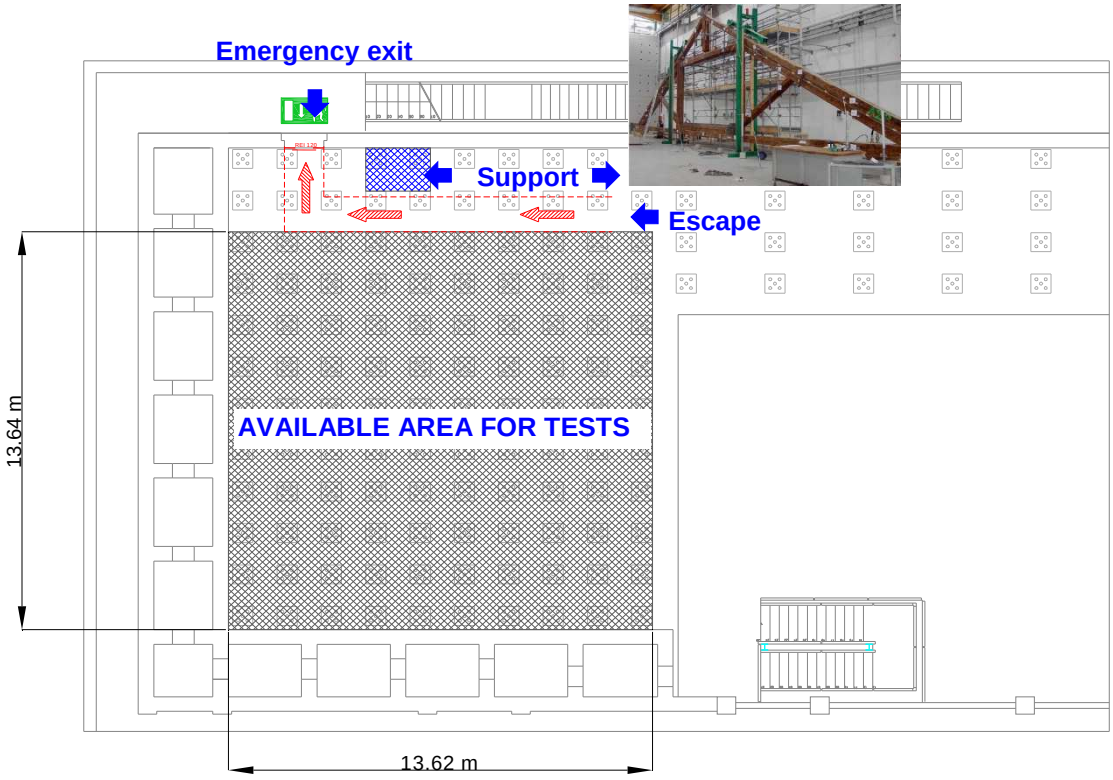

Figure 3-3: Available area for tests

The plan view of the lab shown in Figure 3-2 identify the pattern of the holes in the slab which allow the connection of specimens/counter frames to the slab. The position of these holes identifies possible positions of the columns of the 3-D specimens. The design of the reference

structure was hence carried out by considering the testing availability of all the partners involved in tests and in particular of UTRE.

The 3-D full scale experimental test were performed on a portion of the first floor of the corresponding full-frame, which will be referred to hereinafter as sub-frame. The floor framing plan of the sub-frames for the Symmetric and Asymmetric configurations are represented by the dotted area in Figure 3-4 and Figure 3-5 respectively which dimensions are in agreement with the lab testing facilities.

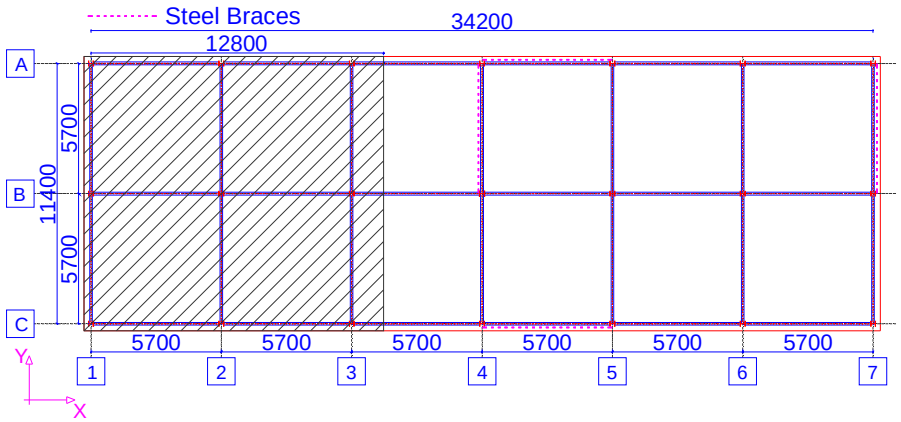

Figure 3-4: Floor Framing Plan - Symmetric Configuration (dimensions in mm)

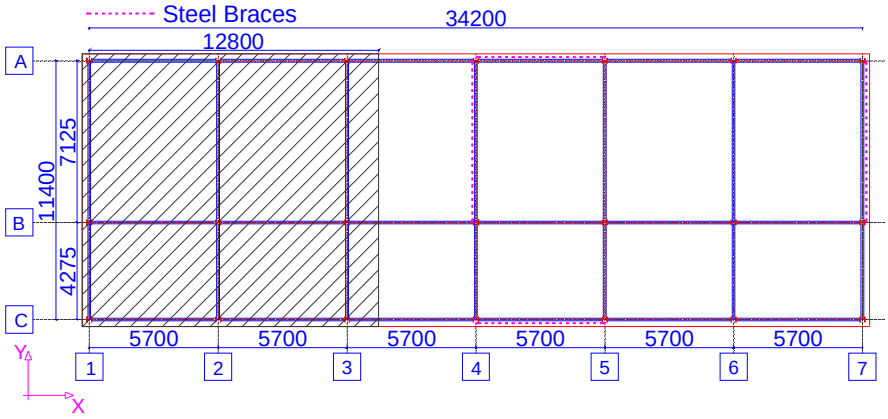

Figure 3-5: Floor Framing Plan - Asymmetric Configuration (dimensions in mm)

The final geometry of the two specimens and the layout of the slab rebars are presented in Figure 3-6. 'Symmetric' Structure. Slab reinforcements. (a) Lower layer; (b) upper layer (dimensions in m). The rebars layout showed in the figures are in agreement with ones calculated for the reference structures (Figure 2-38, Figure 2-39, Figure 2-50 and Figure 2-51).

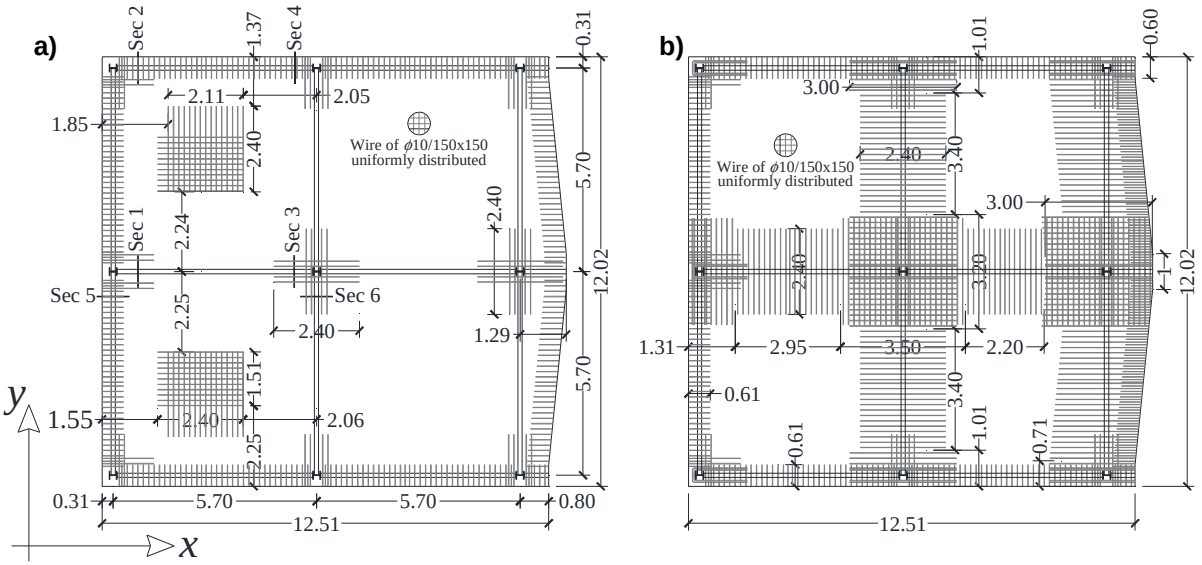

Figure 3-6. 'Symmetric' Structure. Slab reinforcements. (a) Lower layer; (b) upper layer (dimensions in m)

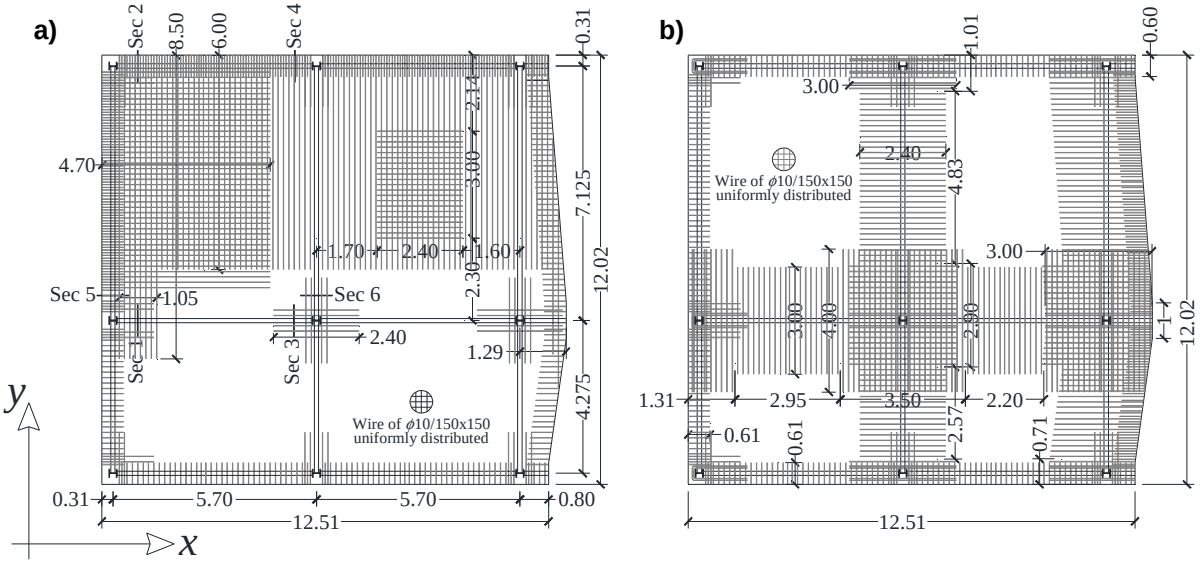

Figure 3-7. 'Asymmetric' structure. Slab reinforcements. (a) Lower layer; (b) upper layer (dimensions in m)

3.1 Numerical analysis of the experimental test

In order to design the experimental tests, refined Finite Element Models of the full-frames and sub-frames were developed by using the Abaqus program [9]; beams and columns are modeled as 'Frame' elements while the slabs are modeled as 'Shell' elements with quadrilateral elements with 4 nodes. The 'Frame' elements are modeled in the position corresponding their central axis, while the 'Shell' elements are modeled in the position corresponding the mid height of the concrete section. The 'Shell' elements are modeled with a constant thickness and, in order to reproduce the real distribution of the rebars in the slabs, accurate partitions and several sections accounting for different dimensions and spacing were adopted. Figure 3-8 show the partitions defined for the 'Symmetric' configuration, while Figure 3-9 refers to the 'Asymmetric' case [ref]. The representation considers the rebars excluding their anchorage length. The rebars

are embedded within the slab and the slab is rigidly connected to the beams through 'TIE' constraints [9]. In the preliminary study, a rigid beam-to-column connection is considered and the columns are fully fixed at the base. The loads are uniformly distributed on the slab and are gradually increased by using a smooth step. Different levels of meshing arrangements for the beams and the slabs have been considering in order to ensure an adequate structural response while minimizing the computational time of the simulations. Meshing of all the parts is carried out using the 'structured' technique. Mesh refinement with an average value of 200 mm has been used.

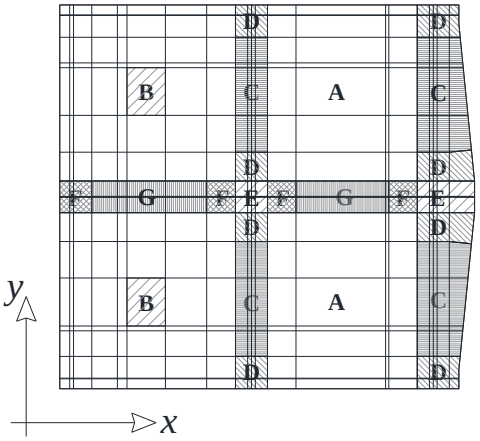

Section	Rebars			
	x bottom	y bottom	x top	y top
A	ϕ10/150	ϕ10/150	ϕ10/150	ϕ10/150
B	2ϕ10/150	2ϕ10/150	ϕ10/150	ϕ10/150
C	ϕ10/150	ϕ10/150	2ϕ10/150	ϕ10/150
D	ϕ10/150	ϕ10/150	(ϕ10+ϕ16)/150	ϕ10/150
E	ϕ10/150	ϕ10/150	(ϕ10+ϕ16)/150	(ϕ10+ϕ16)/150
F	ϕ10/150	ϕ10/150	ϕ10/150	(ϕ10+ϕ16)/150
G	ϕ10/150	ϕ10/150	ϕ10/150	2ϕ10/150

Figure 3-8. 'Symmetric' structure. (a) Concrete slab partitions; (b) slab section properties (measures in mm)

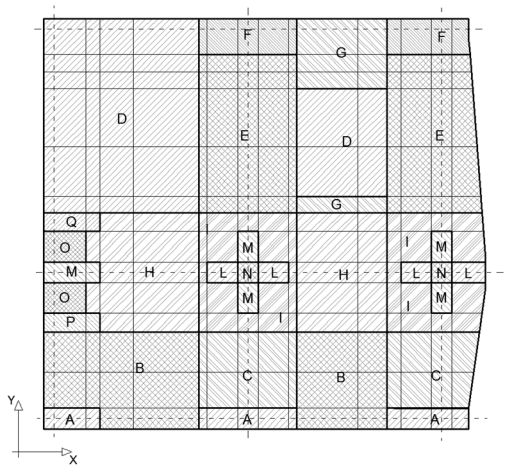

Section	Rebars			
	x bottom	y bottom	x top	y top
A	ϕ10/150	ϕ10/150	(ϕ10+ϕ16)/150	ϕ10/150
B	ϕ10/150	ϕ10/150	ϕ10/150	ϕ10/150
C	ϕ10/150	ϕ10/150	ϕ10/150	ϕ10/150
D	ϕ10/150	ϕ10/150	2ϕ10/150	ϕ10/150
E	ϕ10/150	2ϕ10/150	2ϕ10/150	ϕ10/150
F	ϕ10/150	2ϕ10/150	(ϕ10+ϕ16)/150	ϕ10/150
G	ϕ10/150	2ϕ10/150	ϕ10/150	ϕ10/150
H	ϕ10/150	ϕ10/150	ϕ10/150	2ϕ10/150
I	ϕ10/150	ϕ10/150	(ϕ10+ϕ16)/150	(ϕ10+ϕ16)/150
L	2ϕ10/150	ϕ10/150	(ϕ10+ϕ16)/150	(ϕ10+ϕ16)/150
M	ϕ10/150	2ϕ10/150	(ϕ10+ϕ16)/150	(ϕ10+ϕ16)/150
N	2ϕ10/150	2ϕ10/150	(ϕ10+ϕ16)/150	(ϕ10+ϕ16)/150
O	ϕ10/150	2ϕ10/150	ϕ10/150	(ϕ10+ϕ16)/150
P	2ϕ10/150	ϕ10/150	ϕ10/150	(ϕ10+ϕ16)/150

Figure 3-9. 'Asymmetric' structure. (a) Concrete slab partitions; (b) slab section properties (measures in mm)

The structural steel and the rebars are modeled by an elastic perfectly plastic material model based on the nominal values of the mechanical properties. The Young's modulus, E and the yield stress, fy, are assumed equal to 200 GPa and 450 MPa and to 210 GPa and 355 MPa

for steel B450C and steel S355, respectively. The Poisson's coefficient is assumed equal to 0.3 for both the steel materials. Material non-linearity for the concrete is included in the FE model by the 'Concrete Damage Plasticity' option. The stress-strain relationship are defined in compression according to the Eurocode 2 [3] and in tension according to [10] including the effects of the tension stiffening. Stress-strain relationships for the concrete are reported in Figure 3-10. The von Mises yield criterion coupled with an isotropic hardening is assumed. All the material properties are defined accounting for the true values of stress, σ_t, and plastic strain, $\varepsilon_{t,pl}$ [11]. True stress-strain relationships and the plastic strain can be obtained based on the engineering values by the following equations:

$$\sigma_t = \sigma_{nom}\left(1+\varepsilon_{nom}\right) \tag{1}$$

$$\varepsilon_t = \ln\left(1+\varepsilon_{nom}\right) \tag{2}$$

$$\varepsilon_{t,pl} = \varepsilon_t - \varepsilon_{t,el} = \varepsilon_t - \sigma_t / E \tag{3}$$

where σ_{nom} is the engineering stress, εnom is the engineering strain, σ_t is the true stress, ε_t is the true strain, $\varepsilon_{t,pl}$ is the true plastic strain and $\varepsilon_{t,el}$ is the true elastic strain.

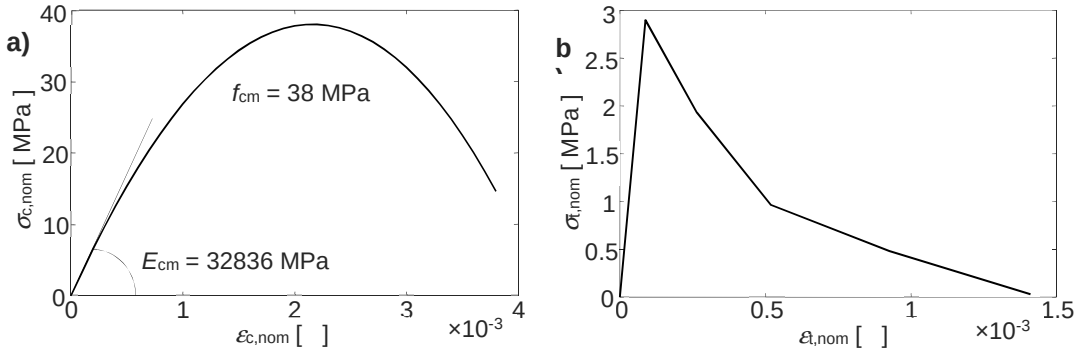

Figure 3-10. Concrete stress-strain relationships. (a) Compression and (b) tension behavior for concrete class C30/37 according to [3] and [10]

The numerical simulations of the tests, performed in ABAQUS [9], follow the three steps of the loading procedure. In the first step, the gravity load is applied on the slab defining the condition before the column's collapse; in the second step the central column is 'removed', while in the third step, additional load is applied onto the slab up to the collapse in order to get an appraisal of the available safety margin. The first step is performed by a static analysis while the second and third steps are performed by quasi-static analyses. The static analysis is performed with the ABAQUS/Standard solver; in this case the central column is fixed at the base and the analysis provides the vertical reaction force of the element. The equilibrium equations are solved using the static general analysis procedure. The standard 'Full Newton' solution technique is adopted together with an automatic incrementation scheme for the application of the loading. In the following steps, the quasi-static analyses are performed with the ABAQUS/Explicit solver which offer advantages while solving large non-linear problems. In the second step the central column is released and the reaction force from step 1 is applied at the base. A force in the opposite direction is increased in order to gradually reduce the force up to zero. In the third step the gravitational load on the slab is gradually increased. In these analyses, the dynamic equilibrium equations are solved using the central difference algorithm; the velocity of the column displacement is calibrated limiting the ratio between the kinetic energy and the internal energy (i.e. ≤ 0.01), ensuring that the dynamic effects are negligible. The response of the full-frame and sub-frame of the symmetric configuration in the three steps is reported in Figure 3-11.

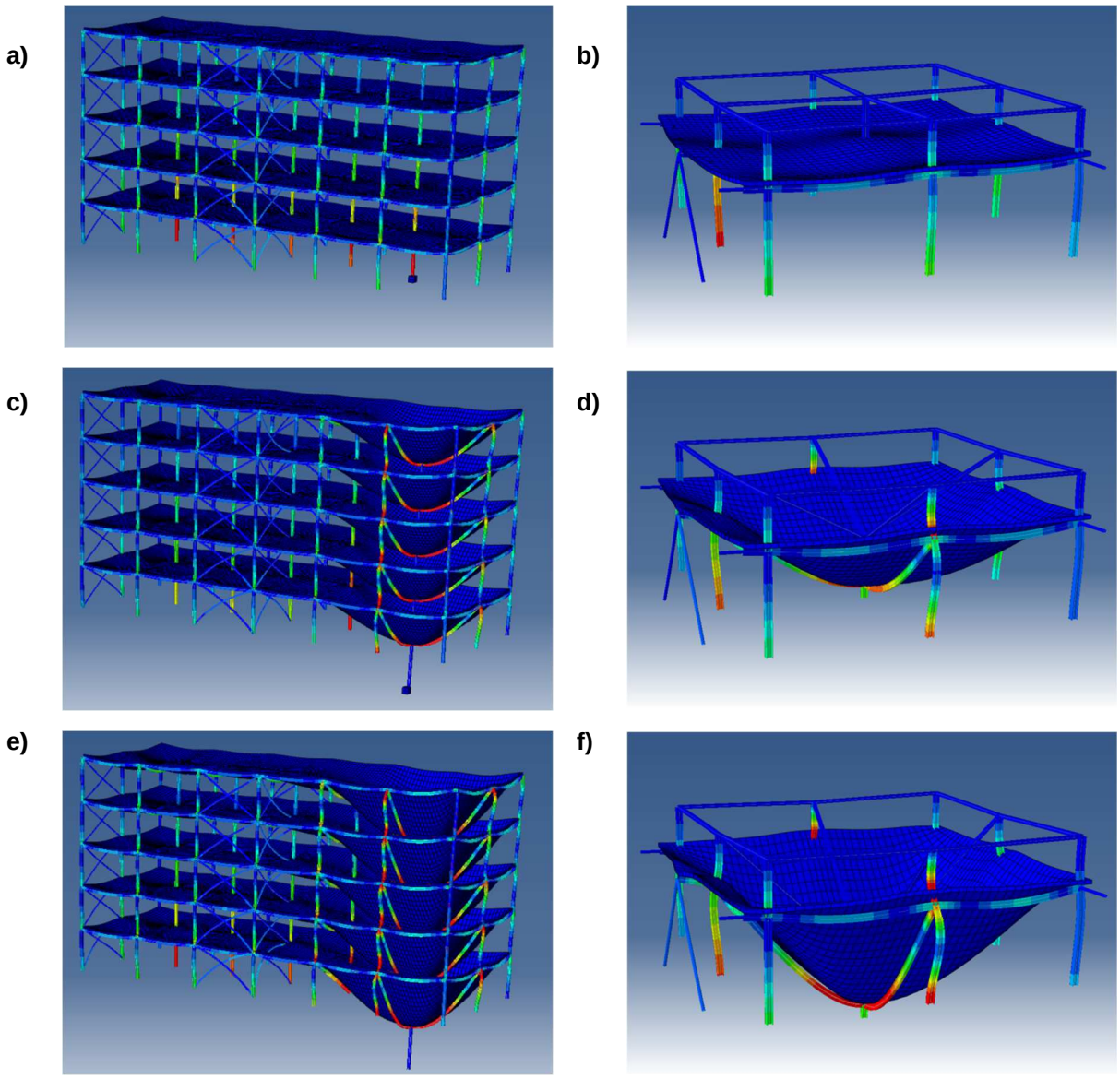

Figure 3-11. Sequence of collapse for the full-frame and sub-frame with the following loading steps: a) and b) Application of gravity load; c) and d) Removal of column; e) and f) Increase of load.

3.1.1 *Sub-frame boundary conditions*

The task of the experimentation is to investigate the behavior of the real structure subjected the collapse of a column. Hence, the sub-frame should be restrained in a way that permits simulation of the presence of the remaining part of the structure and this issue was of primary interest in the preliminary study for the test design.

The sub-frame is 'extracted' from the ground floor of the full-frame and hence the columns are fixed at the strong floor. The columns are longer than the story height, and continue up to the middle height of the second story, where they are connected among them by steel truss elements as represented in

Figure 3-12. This specimen's configuration allows for approximating well the distribution of the moments in the columns and the rotational stiffness of the beam-column joints.

While the definition of the columns' upper restraints was almost immediate, calibration of the connection between beams and slabs with the reaction system required greater attention. Three different restraining options, as illustrated in Figure 3-13, were considered in the analyses, and the main results in terms of deformations and internal forces were compared with the corresponding ones obtained by the analysis of the full-frame. In particular, the adequacy of the boundary restraints is checked by comparing the response at several significant sections of the structure reported in Figure 3-14. In order to limit the length of this report, only the results of the Symmetric configuration are reported and discussed in this section. Similar results have been obtained for the Asymmetric configuration.

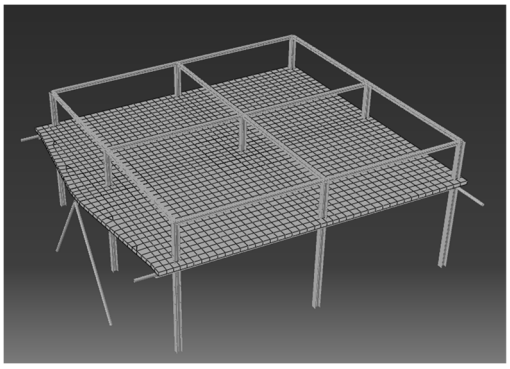

Figure 3-12. Sub-frame for the Symmetric configuration 3-D representation

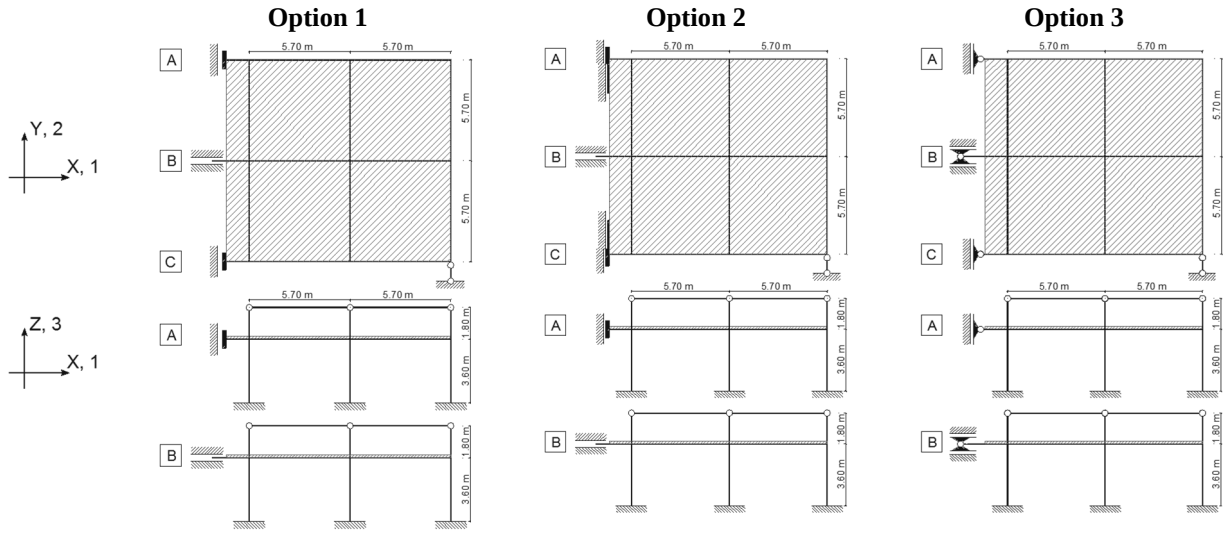

Figure 3-13. Restraining Options for the sub-Frame - Symmetric Configuration

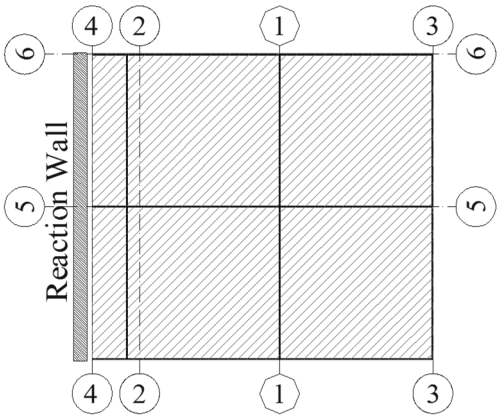

Figure 3-14. Significant Sections used for the comparison - Symmetric Configuration

In the Option 1 and 3, only the steel beams are restrained while the slab is not connected to the reaction wall. The presence of the bracings in full-frame prevents from any significant longitudinal displacement and hence, the relevant d.o.f. U1 is fully restrained in the sub-frame. This d.o.f. is left free at the central beam (B in Figure 3-13) where the vertical and lateral displacements (U2 and U3) are restrained. Besides, in the Option 1, the end rotations of beams A and C about both principal axes (R2 and R3) are restrained, and the central beam's end is restrained against rotations R2 and R3. In the Option 2, in addition to the restraints of the Option 1, also the parts of the slab adjacent to the lateral beams are connected, for a width of 0.5 m, to the reaction wall, restraining all the translational degrees of freedom. The Option 3 is similar to the Option 1 but all the rotations are released.

In order to permit the comparison between the results of the sub-frame and of the full-frame by neglecting the effects of the higher axial load on the columns of the full-frame, concentrated loads are applied on the columns of the sub-frame model and are varied during the analysis in order to simulate the axial force variation of the full-frame. The sequence of the concentrated loads applied on the columns is reported in Figure 3-15.

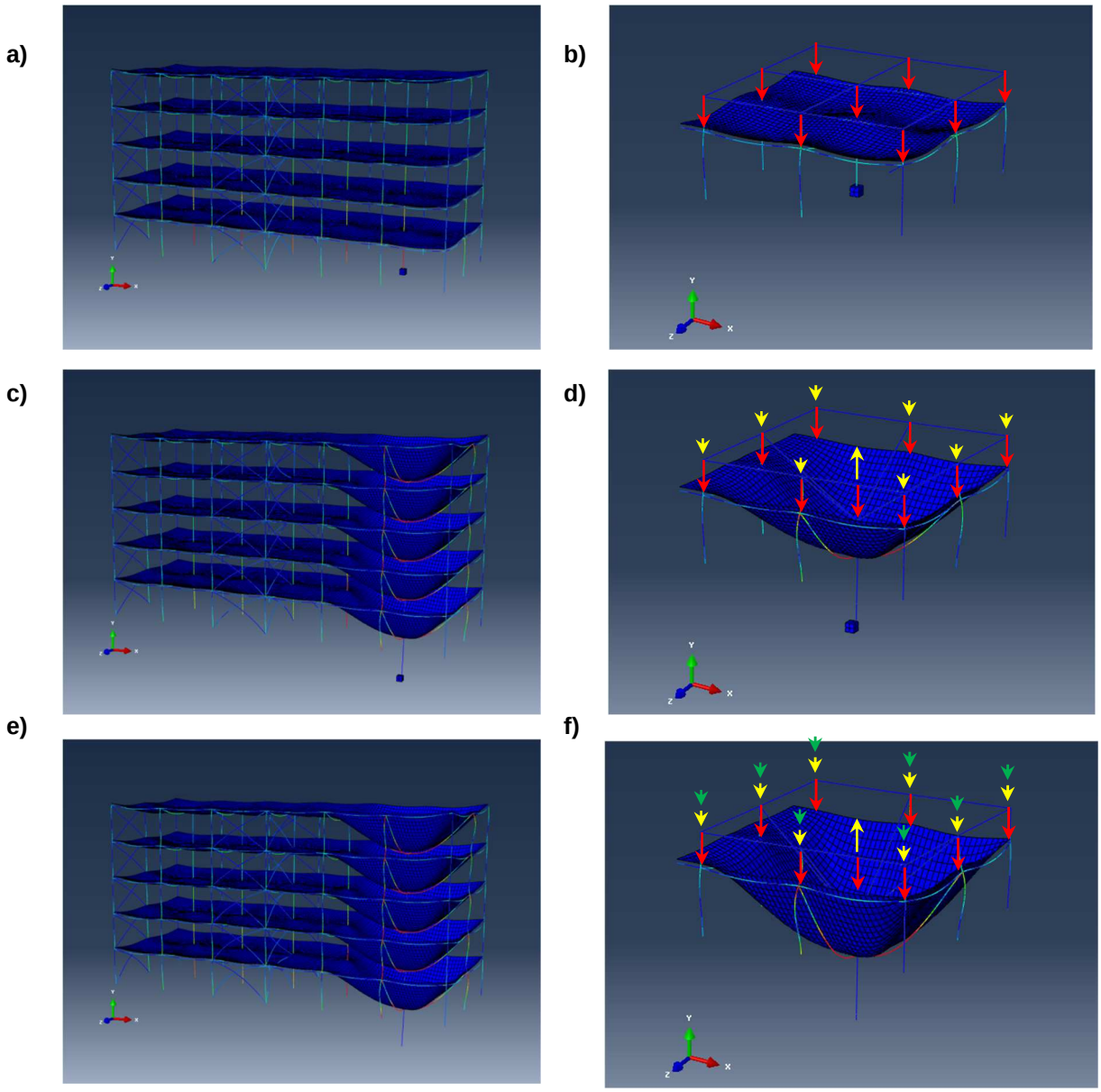

Figure 3-15. Sequence of collapse for the full-frame and sub-frame with the concentrated loads applied on the columns: a) and b) Application of gravity load; c) and d) Removal of column; e) and f) Increase of load

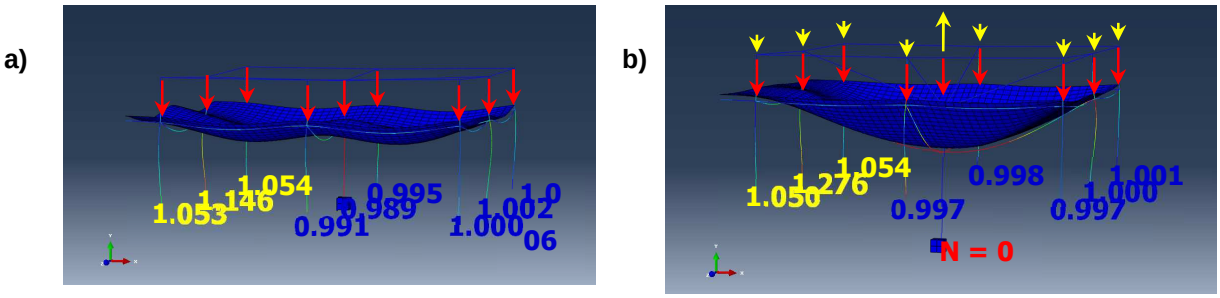

Figure 3-16. The ratios of the axial forces on the columns of full-frame and of sub-frame for: a) first step and b) second step

The ratios of the axial forces on the columns of full-frame and of sub-frame for the first and second steps of the loading sequence are reported in Figure 3-16. It is possible to observe that these values are very close to 1 in all the columns confirming that by this procedure is possible to well approximate the axial force of the full-frame. However, the shear forces in the beams are not simulated and hence the axial forces on the columns of the sub-frame close to the reaction wall are still lower with respect to those of the column of the full-frame.

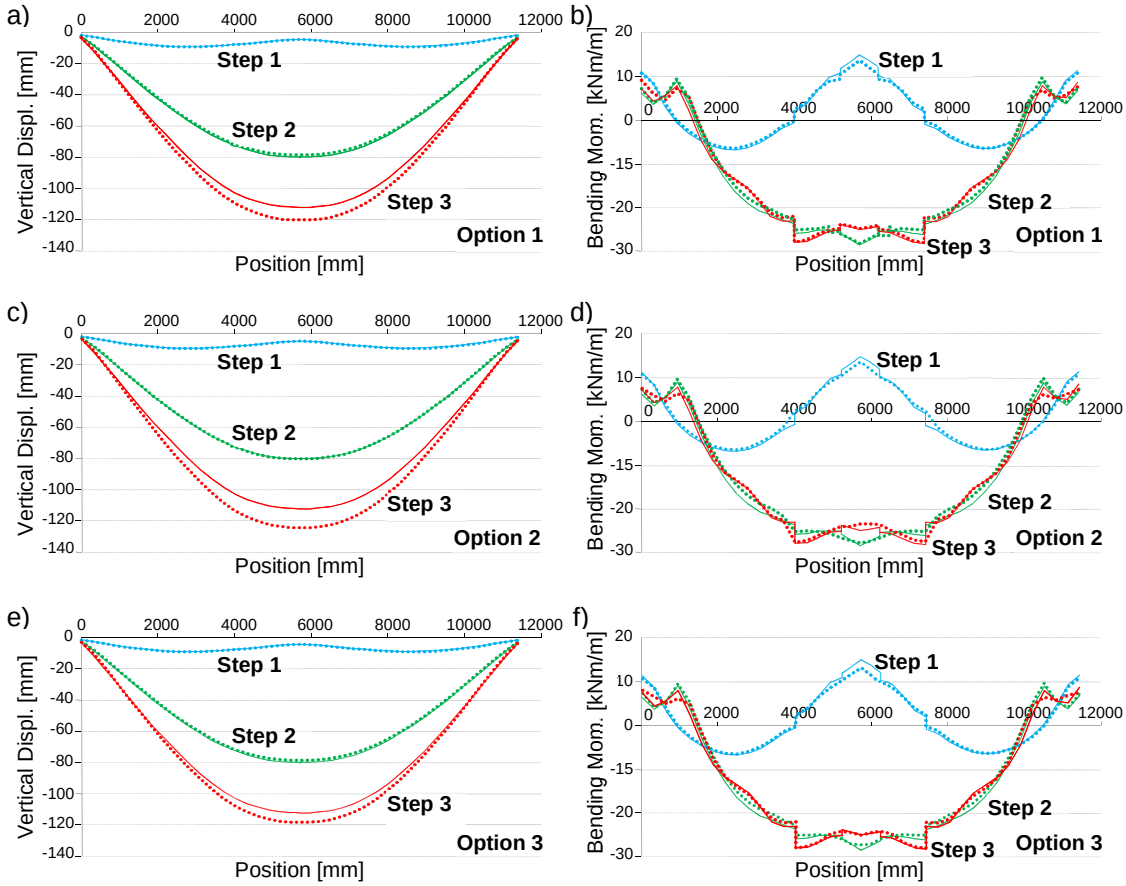

Figure 3-17. Comparison of the Vertical displacements and Bending moments on the Section 1 - Symmetric Configuration

Figure 3-17 shows the comparisons of the vertical displacements and bending moments on the slab positioned on the sections 1 of the sub-frame with one of the three restraining options and the full-frame. The dotted lines indicate the responses of the sub-frames while the continuous line is related to the full-frame. The responses are reported for three steps of the numerical

tests. In the step 1 the gravity load is applied on the slab, in step 2 the central column is completely removed, while in the step 3 the load on the slab is increased with a coefficient equal to 1.3. By looking at Figure 3-17 is possible to observe that there is no significant difference between the results obtained by the three restraining options. Moreover, is possible to observe that all of them are able to approximate more than satisfactorily the behavior of the full-frame in term of displacements and bending moments. Similar results are obtained also by comparing other quantities (i.e. shear, axial force, etc.).

Figure 3-18 shows the comparisons of the vertical displacements and bending moments on the slab positioned on the sections 2 of the sub-frame with one of the three restraining options and the full-frame. Similarly to section 1, also in this case for the first two steps of the analysis the response of the full-frame is well approximated by the sub-frame. Differently, the response of the third step of the analysis is not well captured. It is consequence of the buckling of the central column close to this significant section in the full-frame.

As showed in Figure 3-16 the columns close to this section are more compressed in the full-frame with respect to the sub-frame and the buckling of the central column as showed in Figure 3-19 is not reproduced in the model of the sub-frame. However, this phenomenon is not of interest in this study and there is no significant difference between the results obtained by the three restraining options.

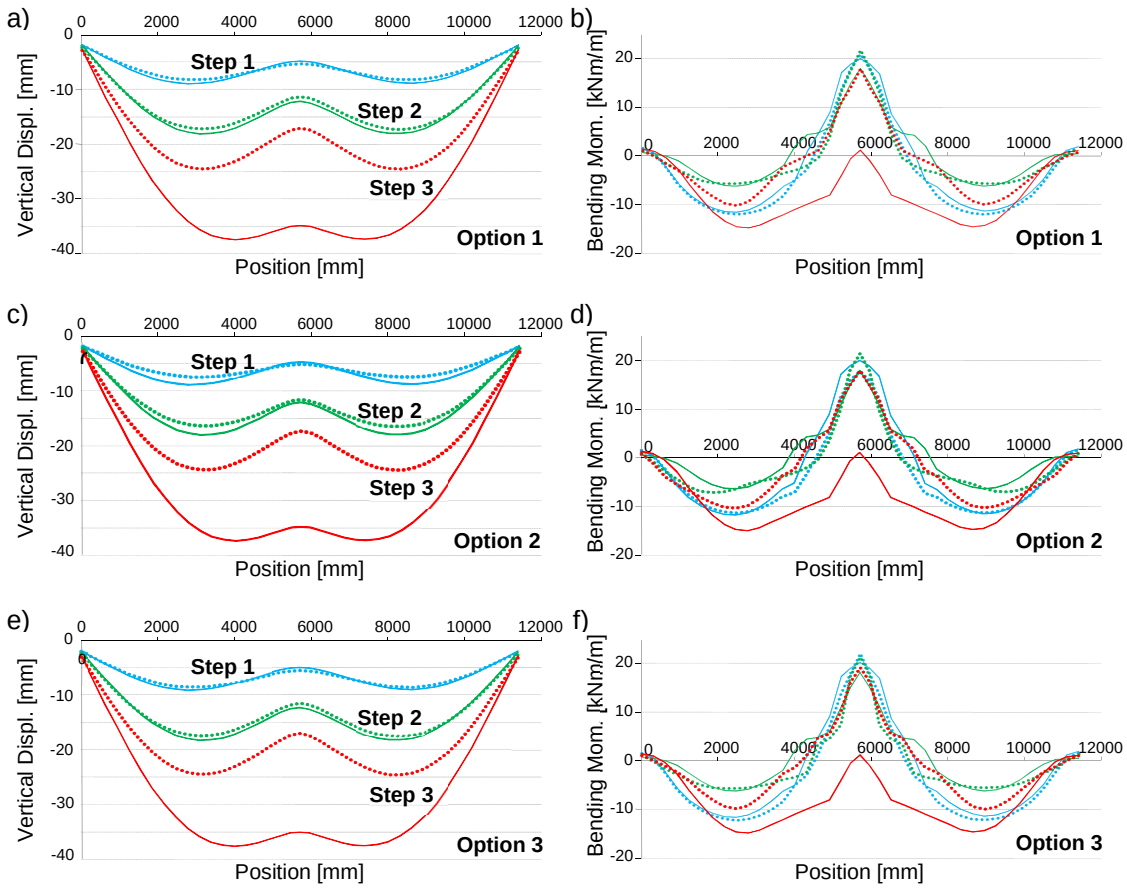

Figure 3-18. Comparison of the Vertical displacements and Bending moments on the Section 2 - Symmetric Configuration

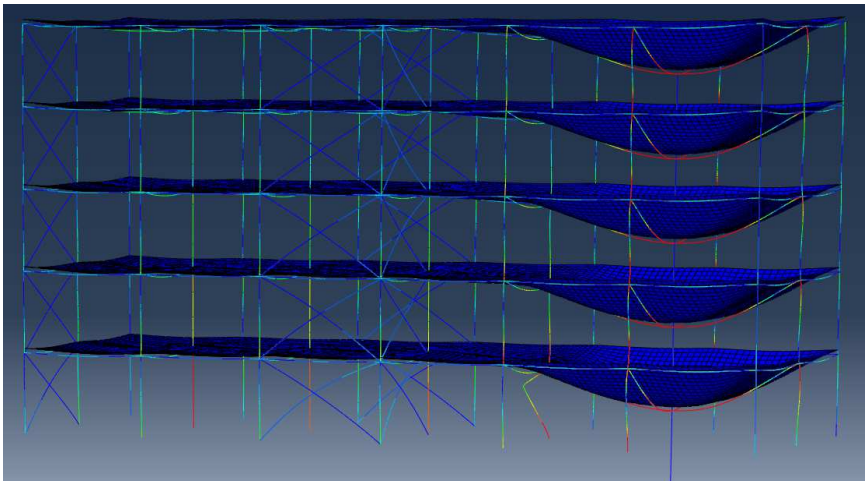

Figure 3-19. Third step of the analysis for the full-frame. Buckling of column.

Figure 3-20 shows the comparisons of the vertical displacements on the slab positioned on the section 4 of the sub-frame with one of the three restraining options and the full-frame. In this section, the response of the sub-frame is strictly related to the restraining option adopted. Figure 3-20 shows that no one of the considered options is able to reproduce well the behavior of the full-frame in this section.

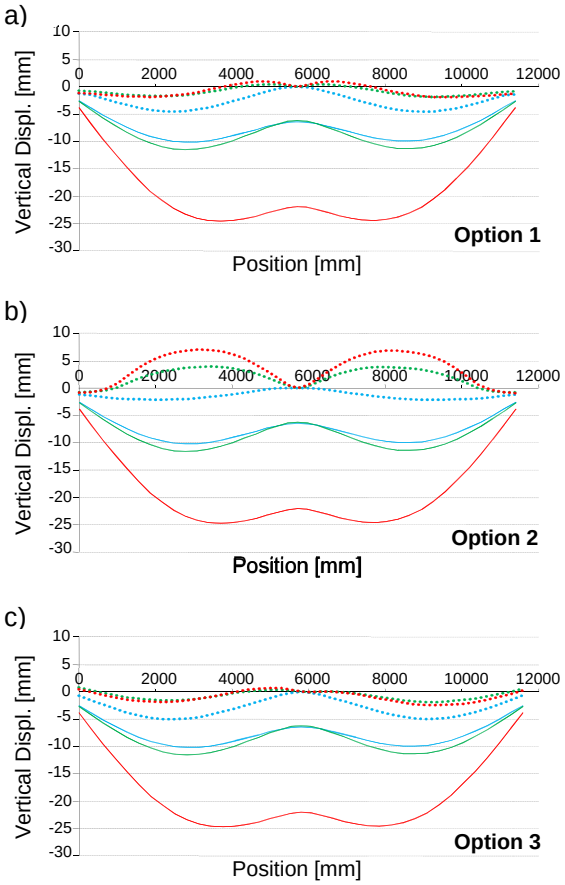

Figure 3-20. Comparison of the Vertical displacements on the Section 4 - Symmetric Configuration

These results indicate that the behavior of the floor subjected to the collapse of the central column is weakly sensitive to the boundary conditions used to reproduce the continuity of the full-frame and that the response on the sections of interest for the experimentation are well reproduced by the sub-frame independently from the response of the external sections. This outcome allows the use of the simplest restraining solution during the test.

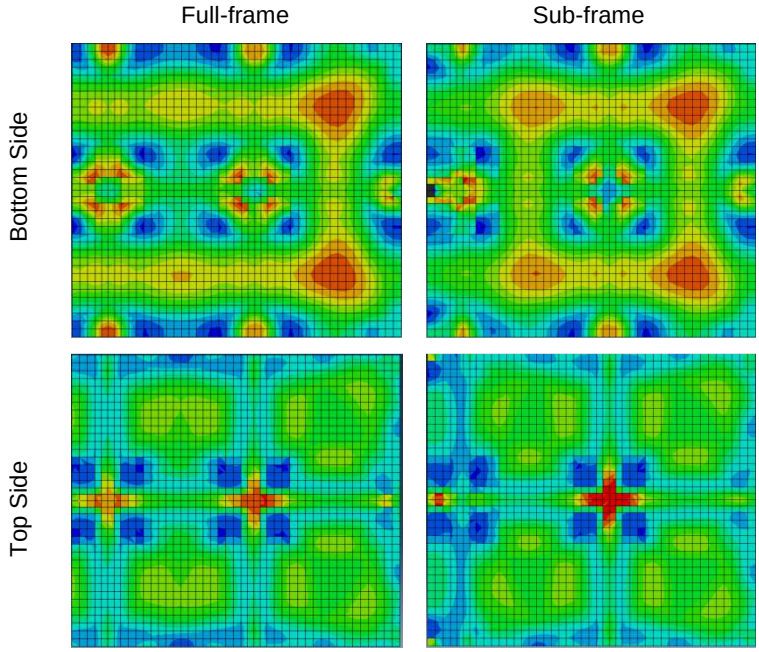

Figure 3-21. Comparison of the Von Mises Stresses on the slab - Step 1 - Symmetric Configuration

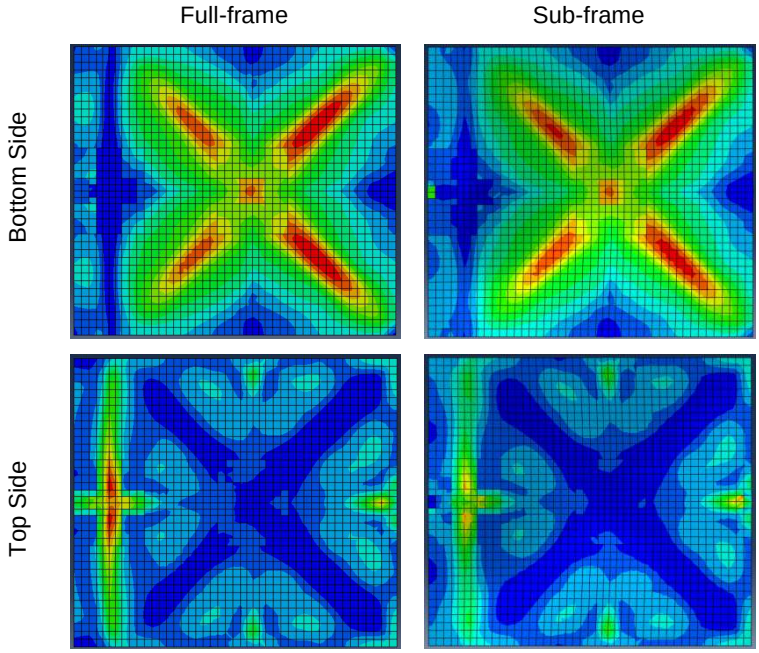

Figure 3-22. Comparison of the Von Mises Stresses on the slab - Step 2 - Symmetric Configuration

Figure 3-22 and Figure 3-22 compare the Von Mises stresses at the bottom and top side of the slab between the full-frame and the sub-frame modeled by using the restraints of Option 3 for

the first and second steps of the analysis. It is possible to observe that the distribution of the stresses obtained in the full-frame is well approximated by the sub-frame model. Analogous results have been obtained also by using the other restraint Options.

3.1.2 *Increase of load after column removal*

While performing the third step of the test's sequence, additional load should be applied onto the slab up to the collapse in order to get an appraisal of the available safety margin. However, application of a distributed load in the frame during the experimental test is not feasible and other solutions have been explored. During the first and second steps the presence of the column is simulated by using a hydraulic ram in which the compression force is gradually reduced down to zero. The hydraulic ram might then used to apply a tension force so simulating the increase of the vertical load in an 'easy' and feasible way. The influence on the frame response of this loading approach was explored by comparing the results of the numerical analysis of the full-frame and of the sub-frame by using the two different loading solutions. The responses are compared in terms of deformations and internal forces at several significant sections of the structure identified in Figure 3-14. However, in order to limit the length of this report, only the results related to section 1 of the Symmetric configuration are reported. Similar results have been obtained for the Asymmetric configuration.

Figure 3-23 shows the comparisons of the vertical displacements and bending moments on the slab positioned on the section 1 of the sub-frame restrained by option 3 with the concentrated load applied in the central column and the full-frame where the increase of load is made by increasing the distributed load on the slab. The dotted lines indicate the responses of the sub-frames while the continuous line is related to the full-frame. The responses are reported for three steps of the numerical tests and in the step 3 the load on the slab is increased with a load factor equal to 1.3. In this case the concentrated force is the equivalent force based on the influence area of the central column. The results for the step 3 indicates that the proposed solution is able to approximate more than satisfactorily the behavior of the full-frame in term of displacements (with an error of 1.5 %) and bending moments. Similar results were obtained also for the other 'significant' sections and by comparing other quantities (i.e. shear, axial force, etc.). The analyses demonstrate that is possible to apply a concentrated force in the central column to increase the vertical load during the test in order to investigate the available safety margin.

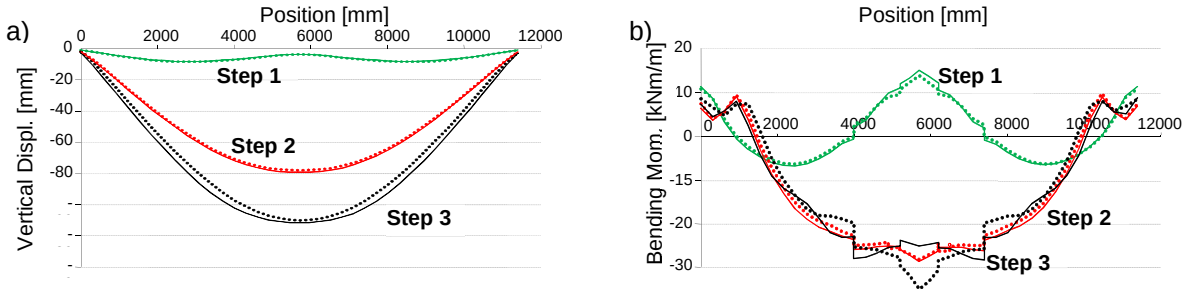

Figure 3-23. Comparison of the vertical displacements and bending moments of the Section 1 - Symmetric configuration

3.2 Design of the test setup

The numerical analysis showed that the behavior of the floor subjected to the collapse of the central column observed in the full-frame can be well simulated in the sub-frame by applying the boundary conditions reported in Figure 3-24. Only the steel beams are restrained while the slab is not connected to the reaction wall. The longitudinal displacement is fully restrained in the

lateral beams (joints A and C). This d.o.f. is left free at the central beam (B in Figure 3-24) while d.o.f. U2 and U3 are restrained. In all the connections, the rotations are released.

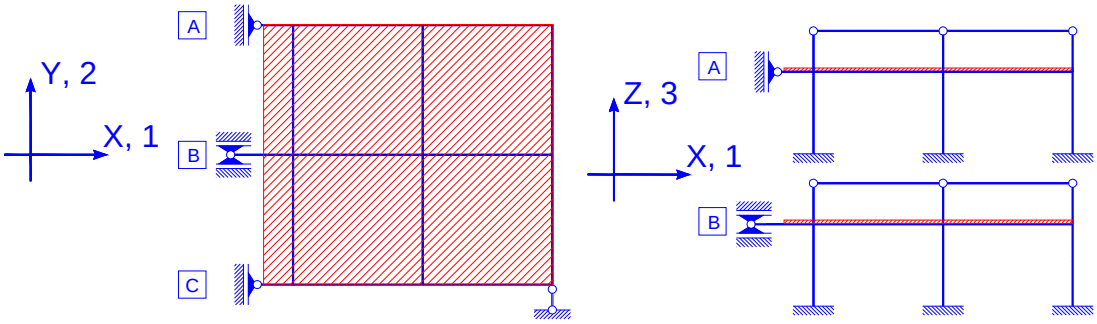

Figure 3-24. Boundary conditions for the sub-frame - Symmetric Configuration

Since the rotations are not restrained, the boundary conditions reported in Figure 3-24 have been obtained by using truss elements. The same elements of the test setup are going to be employed for both the Symmetric and Asymmetric configurations, hence, they have been designed by considering the worst condition among the two cases.

The specimens will be built inside the laboratory. Figure 3-25 and Figure 3-26 report the 3-D representation of the sub-frame and the relative position with respect to the reaction walls including the elements employed to reproduce appropriate boundary conditions.

Figure 3-27 shows the plan view of the experimental test for the Symmetric configuration while Figure 3-28 up to Figure 3-32 report the relative sections. These Figures include the indications of the lateral supports, of the central support, of the hydraulic ram and of the base supports.

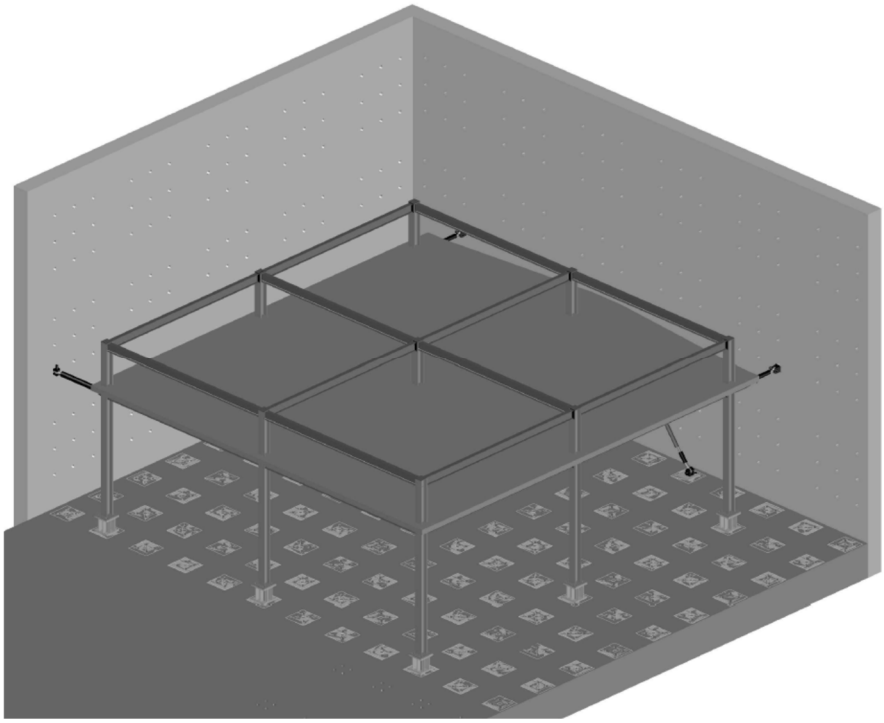

Figure 3-25. Symmetric 3-D specimen

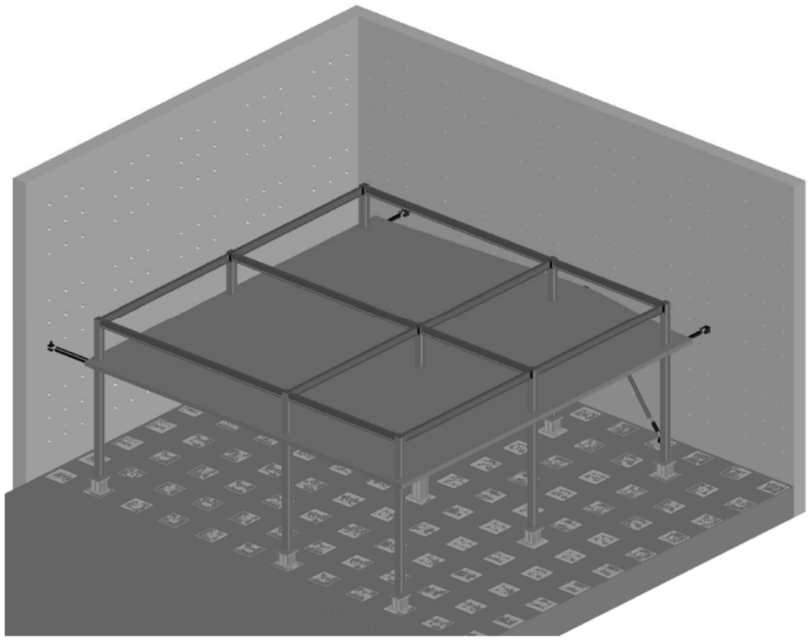

Figure 3-26. Asymmetric 3-D specimen

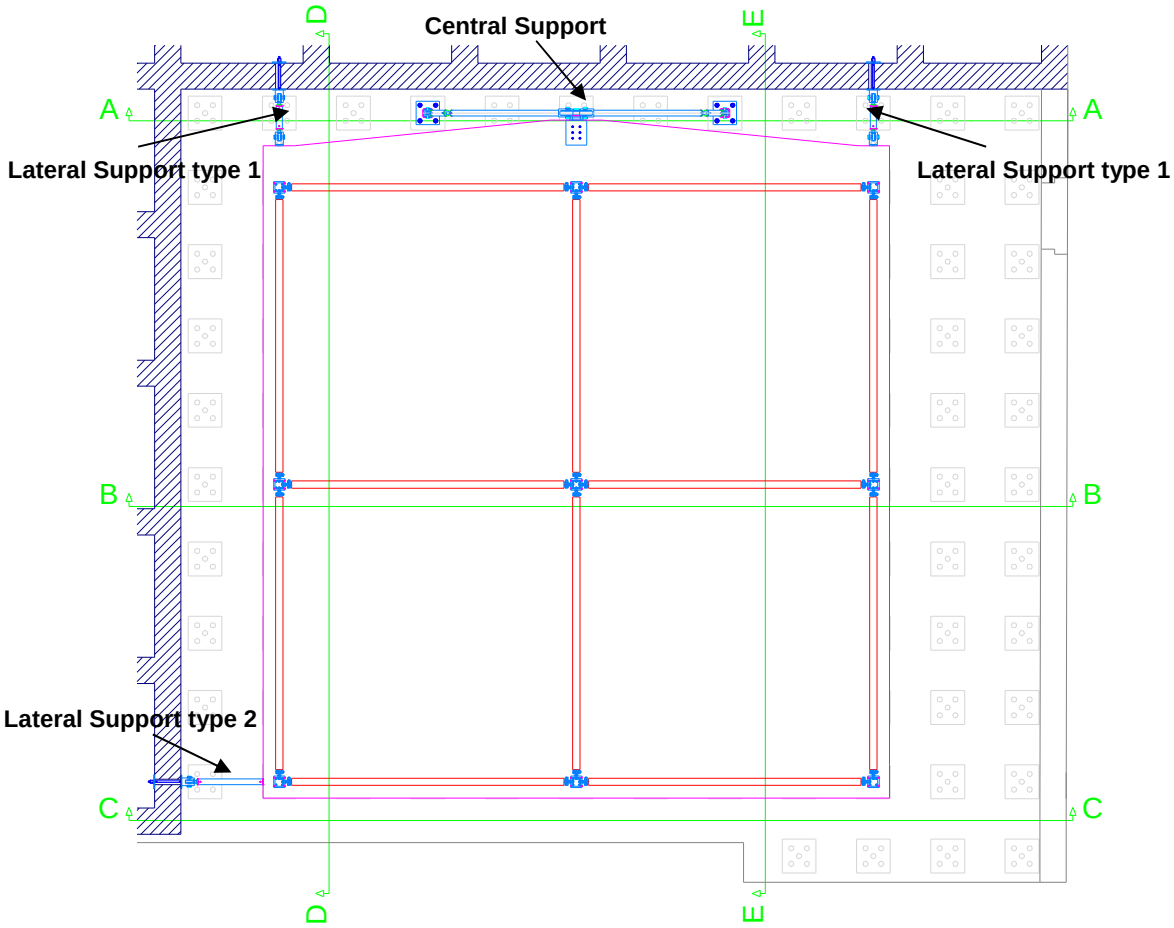

Figure 3-27. Plan View of the Experimental Tests for the Symmetric Configuration

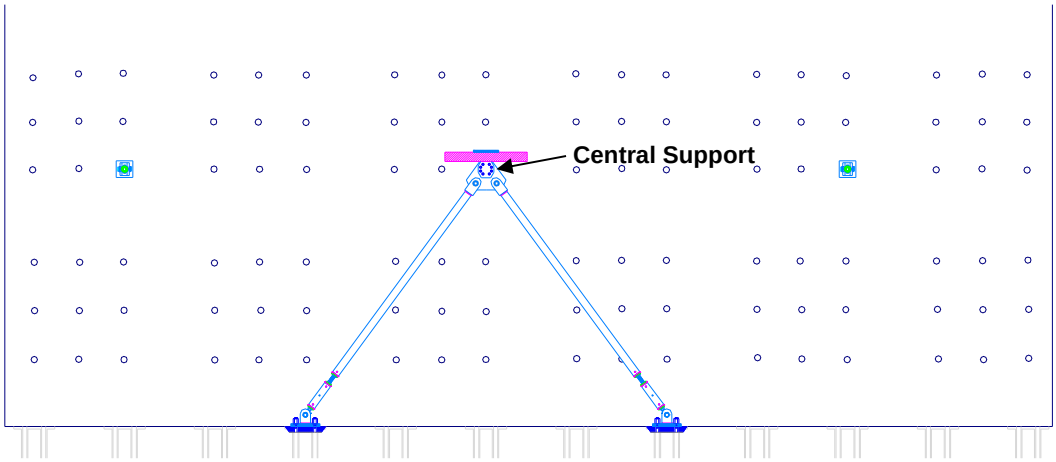

Figure 3-28. Section A-A of the experimental test setup for the Symmetric Configuration

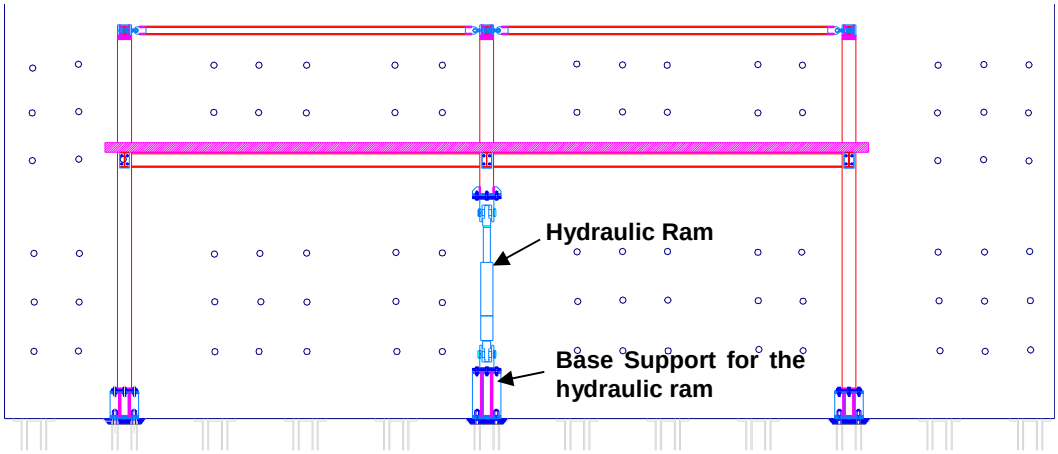

Figure 3-29. Section B-B of the experimental test setup for the Symmetric Configuration

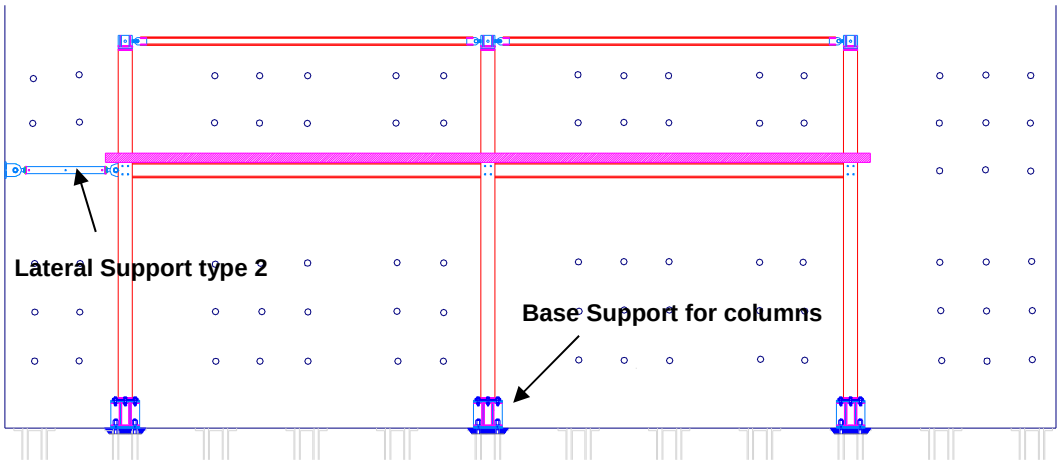

Figure 3-30. Section C-C of the experimental test setup for the Symmetric Configuration

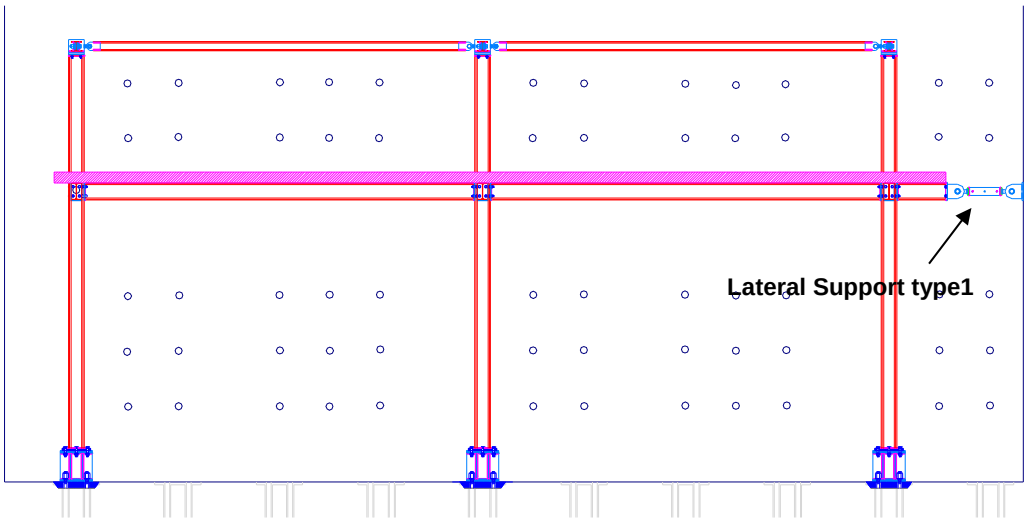

Figure 3-31. Section D-D of the experimental test setup for the Symmetric Configuration

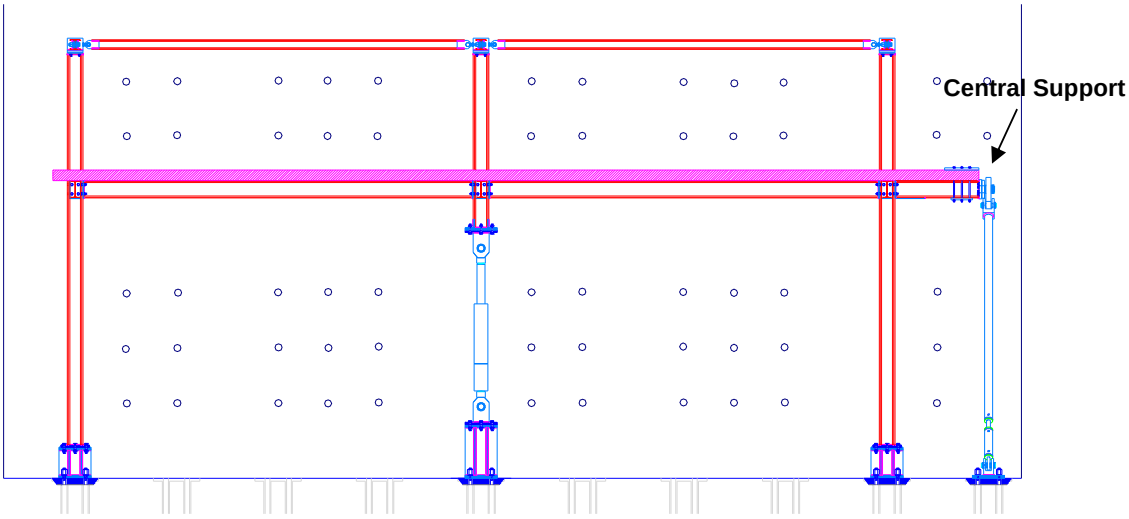

Figure 3-32. Section E-E of the experimental test setup for the Symmetric Configuration

3.2.1 *Restraints of the lateral beams*

The lateral supports are identical with the only difference that the lateral support type 2 is longer. Lateral support type 1 is reported in Figure 3-33. These connections are made by coupling two yokes and rod ends which are connected respectively to the counterwall from one side and to the steel beam form the other side. The rod ends are connected by a tubular steel element by a coupling system that permits the regulation of the length of the elements while assembling the test setup. The rod ends have the rotation that is fully released in the principal direction, while, in the other direction only a rotation of 6 degrees is permitted as reported in Figure 3-34. This solution have been adopted since the numerical analysis showed that in this direction the demand in terms of rotation is lower than 6 degrees.

Both the lateral supports have been designed to support a force in traction of 250 kN.

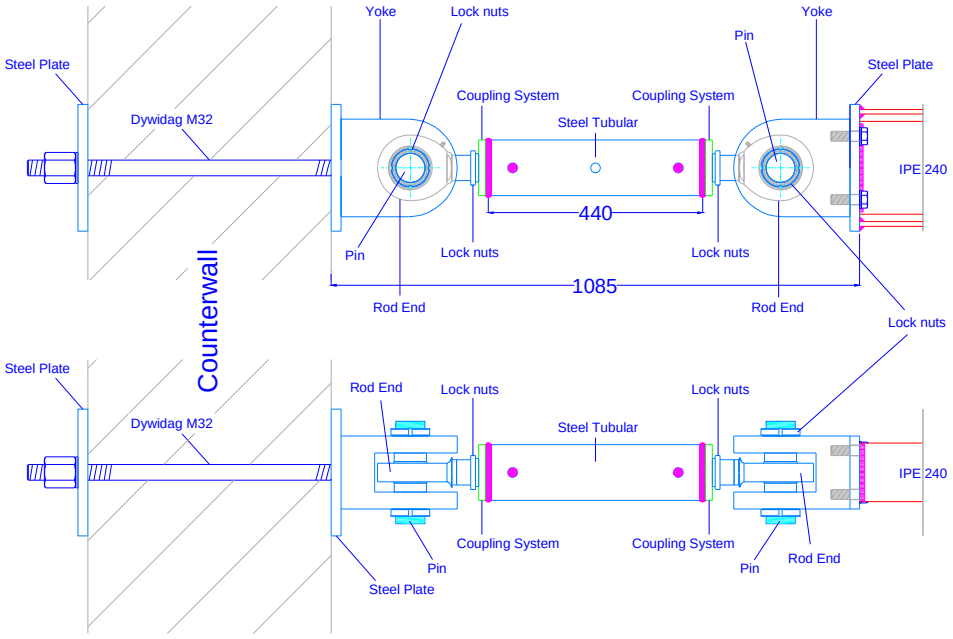

Figure 3-33. Lateral Support type 1

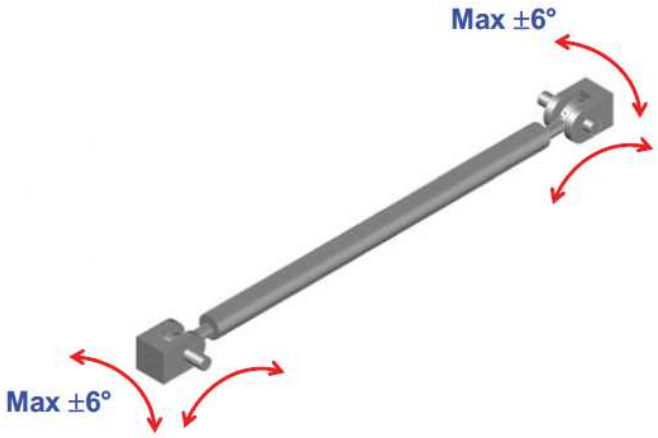

Figure 3-34. Behaviour of Lateral Supports

3.2.2 *Restraints of the central beam*

The central connection is made by two braces which restrain the vertical and the in plane lateral displacement of the central beam as shown in Figure 3-35. Differently, the out of plane lateral displacement is released. The braces are connected to the strong floor and to a steel plate in which is connected the central beam. Figure 3-36 reports a detailed representation of a single brace. The connection with the strong floor is made by yokes and rod ends while the steel plate in the top is equipped with spherical roller bearings in order to permit the connection with the yokes. In this case the braces are composed by two tubular steel elements as can be observed in Figure 3-36. The shorter element has been introduced in order to permit the length regulation of the brace. Also in this case the rod ends have the rotation that is fully released in the principal direction, while, in the other direction only a rotation of 6 degrees is permitted.

The actions on the steel braces have been obtained by the Abaqus model. Figure 3-37 and Figure 3-38 show the axial forces on the diagonal braces of the central joint restraint system

respectively for the Symmetric and Asymmetric frame. The braces of the central supports have been designed to support a force in traction of 250 kN.
The shear force on the central beam transmitted by the central joint restraint system is reported in Figure 3-39.

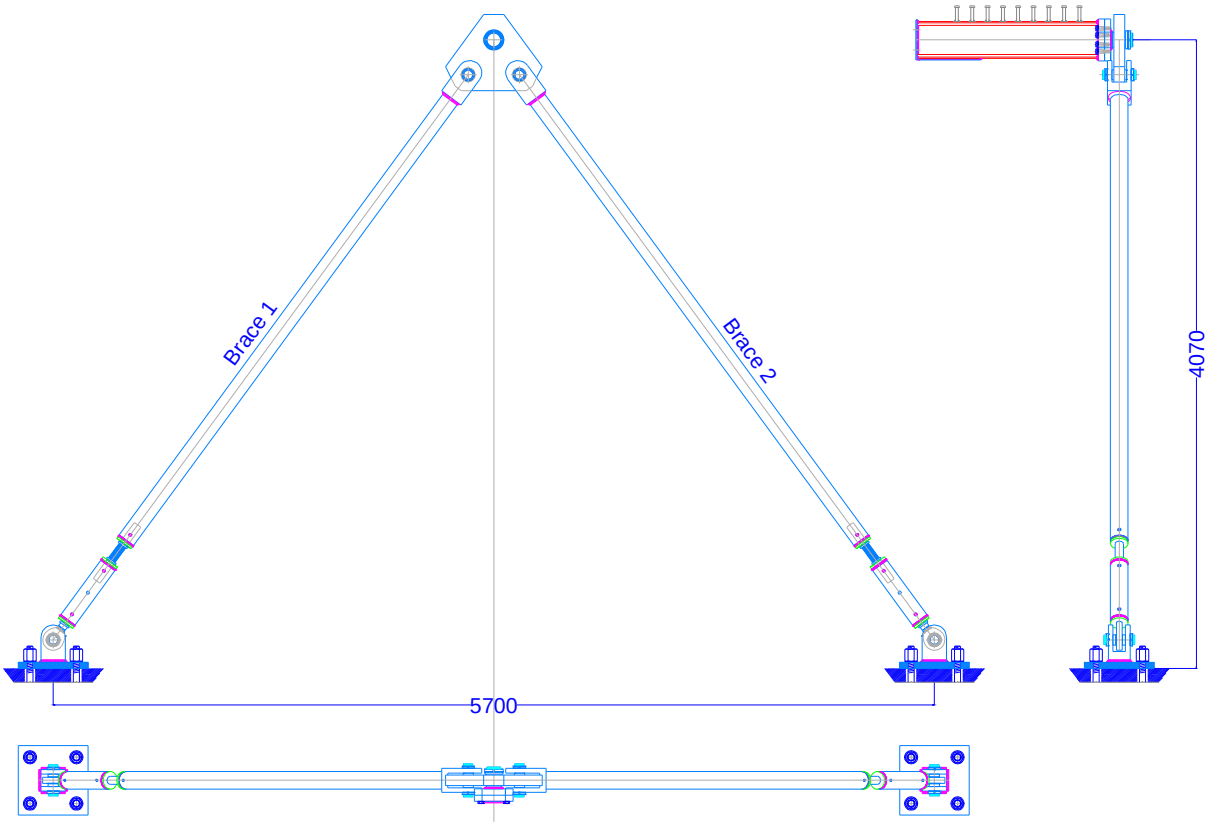

Figure 3-35. Central Support

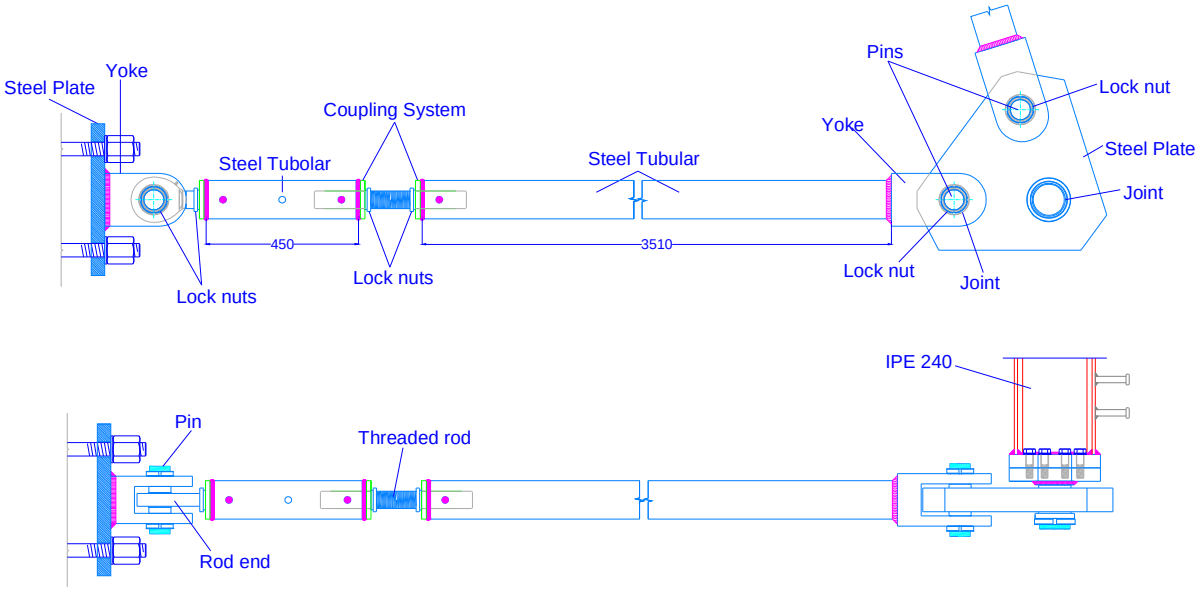

Figure 3-36. Central Support - One brace

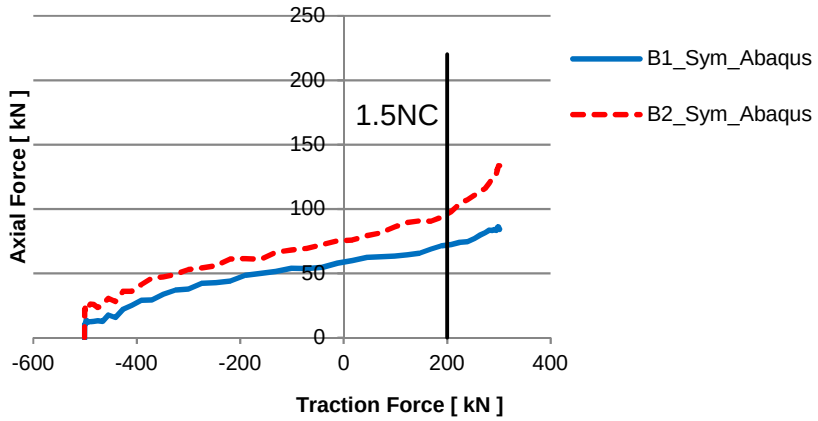

Figure 3-37. Axial Forces on the diagonal braces of the central joint restraint system of the Symmetric Frame

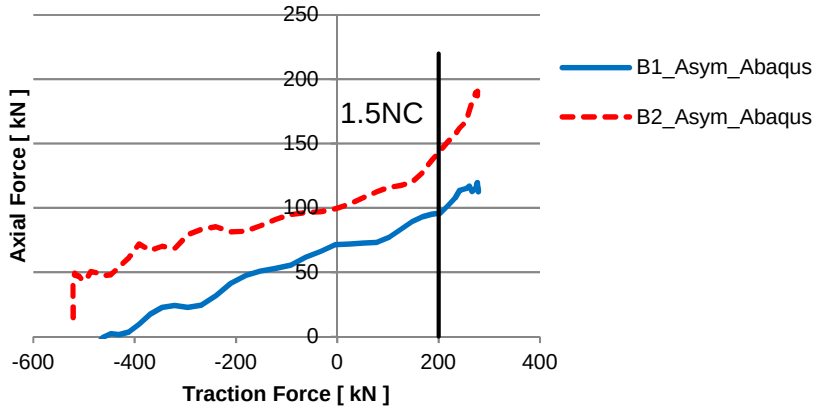

Figure 3-38. Axial Forces on the diagonal braces of the central joint restraint system of the Asymmetric Frame

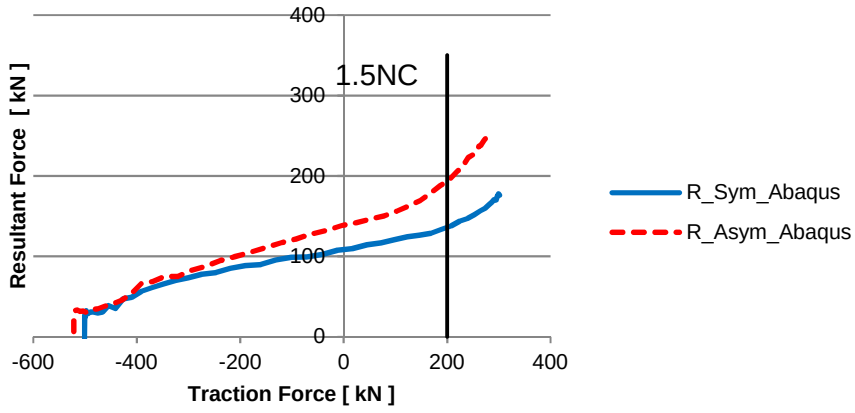

Figure 3-39. Resultant Vertical Force transmitted by the central joint restraint system

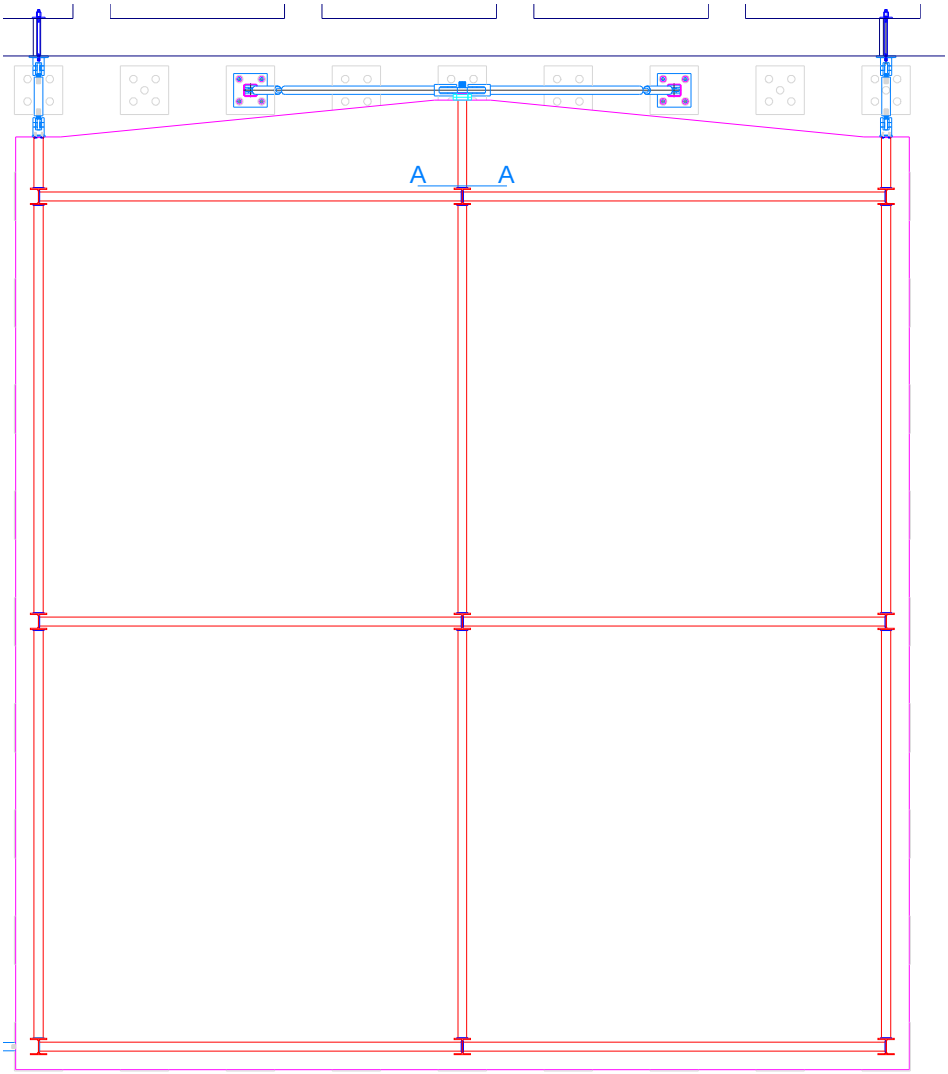

Figure 3-40. Symmetric Frame in the Laboratory. Section A-A

The forces on section A-A as illustrated in Figure 3-40 have been obtained as Free Body Cut in Abaqus. The evaluation of the bending moment on the composite section A-A is made by combining the actions of the beam and of the slab.

$M_{Ed} = 186.909\ kNm$

In order to achieve an adequate safety margin the lower flange of the beam is stiffened with a welded steel plate. The dimensions of the section of the steel plate are 10 x 90 mm^2.

3.2.3 *Column Supports*

As can be observed from Figure 3-29, the central column is supported by a hydraulic ram. The hydraulic ram is introduced in order to permit simulation of the collapse of the central column, and it is arranged with a load cell to monitor the forces. The ends of hydraulic ram and load cell are pinned to the column from one side and to a base support from the other side. These connections, similarly to the other supports previously described are made by using yokes and rod ends.

Figure 3-41 reports the arrangement of the hydraulic ram. The hydraulic ram has a capacity in pulling of 600 kN and all the connecting parts have been designed to resist of this force.

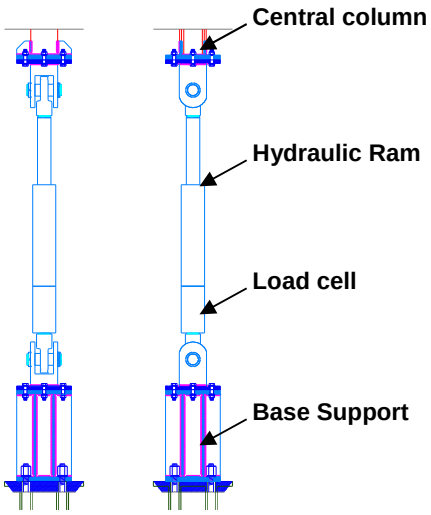

Figure 3-41. Arrangement of the Hydraulic Ram

Both, the hydraulic ram and all the columns are connected with base supports connected to the strong floor by Dywidag bars. Figure 3-42 give a 3-D representation of the base supports.

Figure 3-42. Base support a) for the hydraulic ram, b) for the columns

3.2.4 *Column Supports*

Moreover, as can be observed by the sections, the columns are longer than the story height, and continue up to the middle height of the second story, where they are connected among them by steel elements (HEB 140).

Figure 3-43 reports the central connection of the crowing beams.

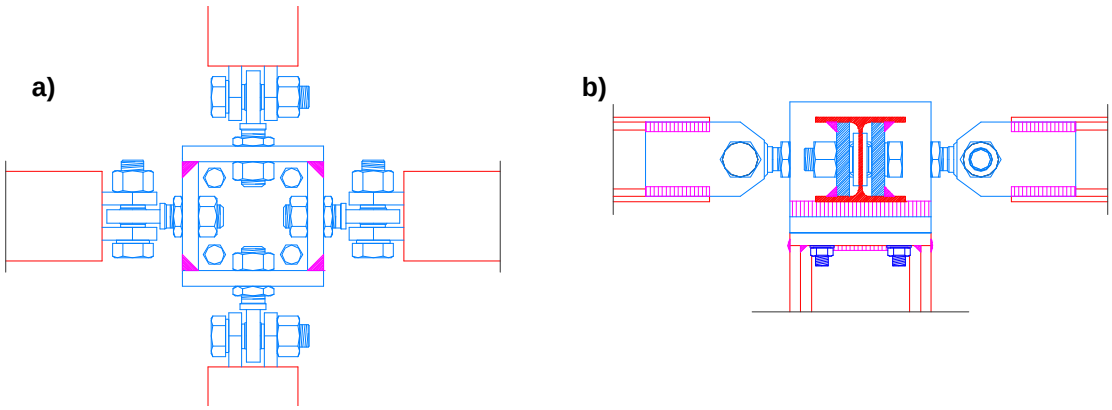

Figure 3-43. Central connection of the crowning beams. a) plan view, b) lateral view

Similar arrangement of the test is going to be employed also for the asymmetric configuration. Figure 3-44 reports the plan view of the experimental test for the symmetric and asymmetric structure.

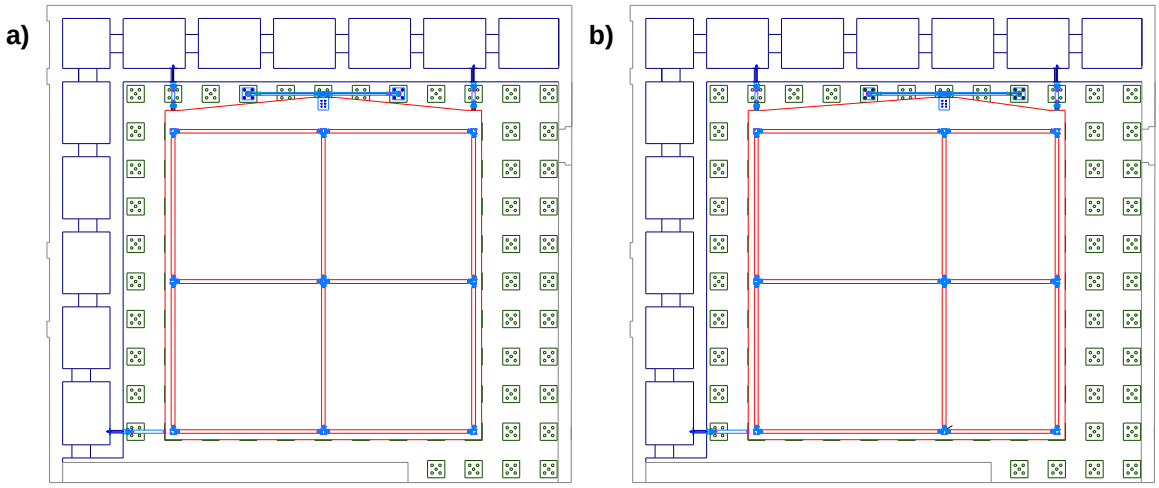

Figure 3-44. Plan View of the Experimental Tests for the a) Symmetric and b) Asymmetric Configuration

4 PRODUCTION OF THE SPECIMENS

In this section, a list of the pieces produced for the construction of the two specimens is given. All the drawings are reported in the annexes A-C.

Depending on the material to be provided, the material was provide by ArcelorMittal, local fabricators and local companies.

4.1 Steel components

Table 4-1 summarises the steel components needed for the construction of steel skeleton of the full-scale specimens.

Table 4-1. Summary of the steel components for the steel skeleton of the full-scale specimens

DESCRIPTION	DRAWING NAME	NUMBER OF PIECES	SPEC. CONFIGURATION	
			Symmetric	Asymmetric
Summary of the steel components	FST 01	-	X	X
COLUMNS TYPE 1				
Steel profile HEB220 length 5500mm	FST 02-09	18	X	X
Steel plate type B 400x400x30mm	FST 03-09	18	X	X
Steel plate type C 220x220x20mm	FST 03-09	18	X	X
Column assembly	FST 09	-	X	X
BEAMS				
Beam type 1 Steel profile IPE240 length 5460mm	FST 04	12	X	X
Beam type 2 Steel profile IPE240 length 5670mm	FST 05	6	X	
Beam type 3 Steel profile IPE240 length 7095mm	FST 06	3		X
Beam type 4 Steel profile IPE240 length 4246mm	FST 07	3		X
Beam type 5 Steel profile IPE240 length 1500mm	FST 08	6	X	X
Steel plate type A	FST 03-04-05-06-07-08	54	X	X

Figure 4-1and Figure 4-2 provide a plan view of the two full-scale specimens (steel skeleton) which allows identifying the position of the various steel components.

The profiles needed for the steel skeleton of both the specimens (Annex A) were produced by ArcelorMittal.

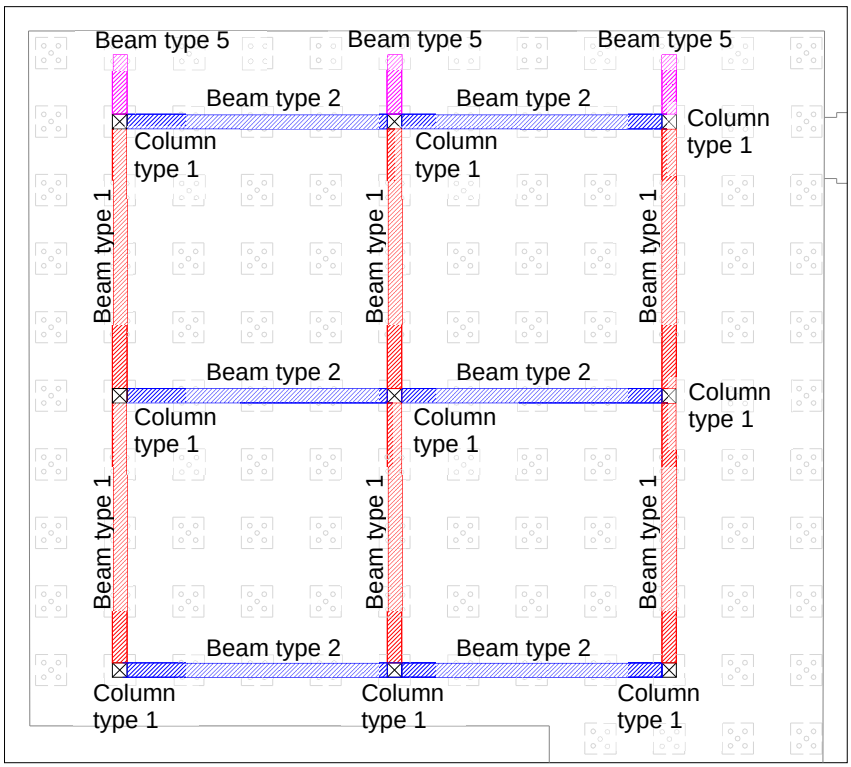

Figure 4-1. Steel profiles for the symmetric full-scale specimen

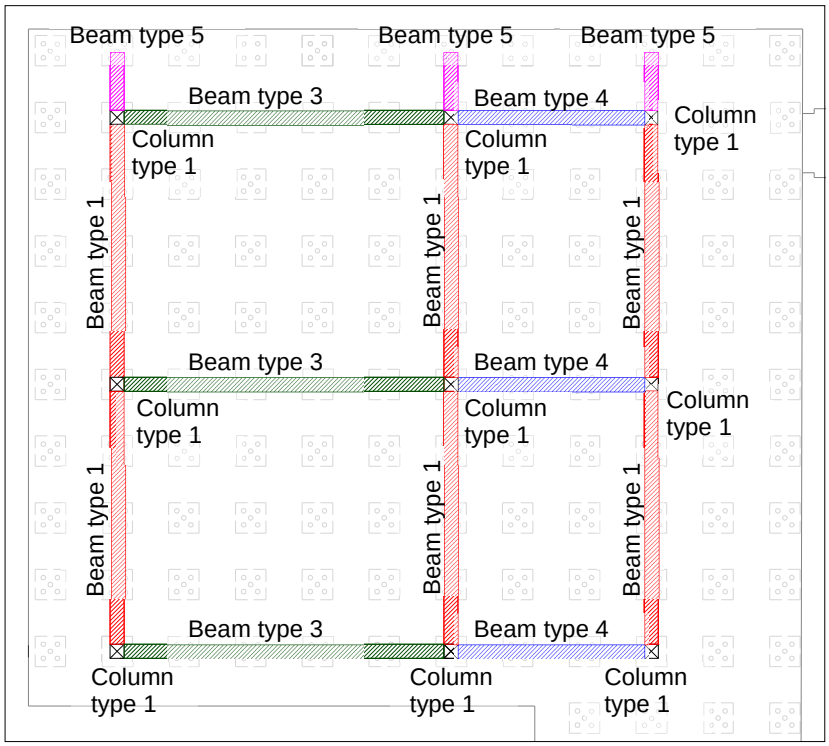

Figure 4-2. Steel profiles for the asymmetric full-scale specimen

4.2 Restraints

In order to reproduce the effect provided by the remaining part of the structure and the base connections, the specimens will be restrained to both the floor slab and the vertical walls of the laboratory. Ai this aim suitable restraints were identified trough FE numerical investigations and accordingly designed. Furthermore, the columns of the specimens, at their upper ends, will be connected together in order to reproduce the effect provided by the levels of the structure above the one considered in the tests. Figure 4-3, Figure 4-4 and Figure 4-5 allow identifying the position of the restraints.
The main drawings related to the restraints are summarised in Table 4-2 and collected in Annex B. The restraints (Annex B) were produced by local fabricators.

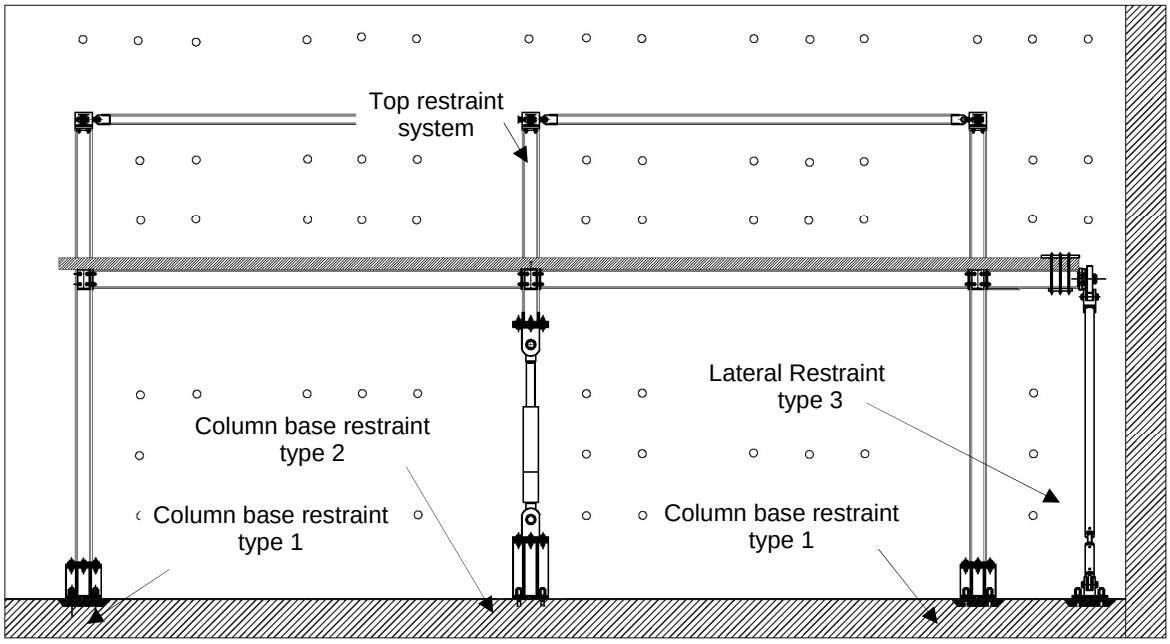

Figure 4-3. Restraints configuration for the full-scale specimens

Table 4-2. Summary of the restraints

DESCRIPTION	DRAWING NAME	NUMBER OF PIECES	SPECIMEN'S CONFIGURATION	
			Symmetric	Asymmetric
RESTRAINTS AT THE COLUMN'S BASE				
Column Base Restraint type 1	CBR1	8	X	X
Column Base Restraint type 2	CBR2	1	X	X
LATERAL RESTRAINTS				
Lateral Restraint type 1	LR1	1	X	X
Lateral Restraint type 2	LR2	2	X	X
Lateral Restraint type 3	LR3	1	X	X
TOP COLUMN RESTRAINTS				
Top connection type 1	TC1	1	X	X
Top connection type 2	TC2	4	X	X
Top connection type 3	TC3	4	X	X

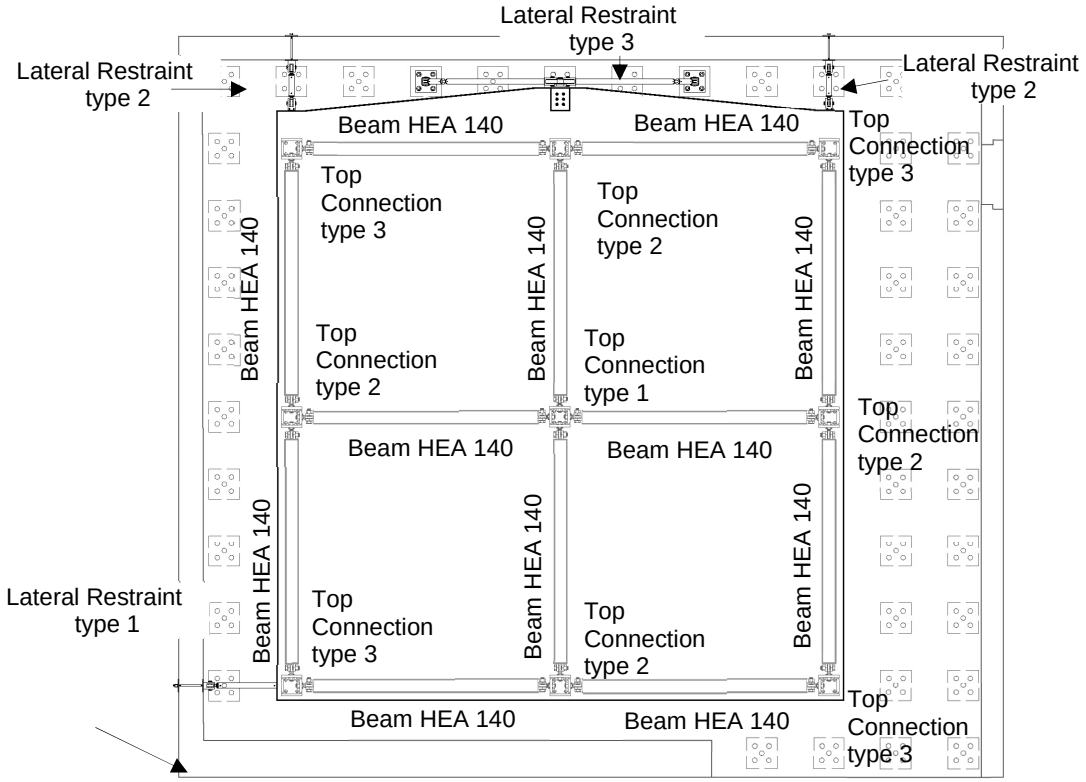

Figure 4-4. Restraints for the symmetric full-scale specimen

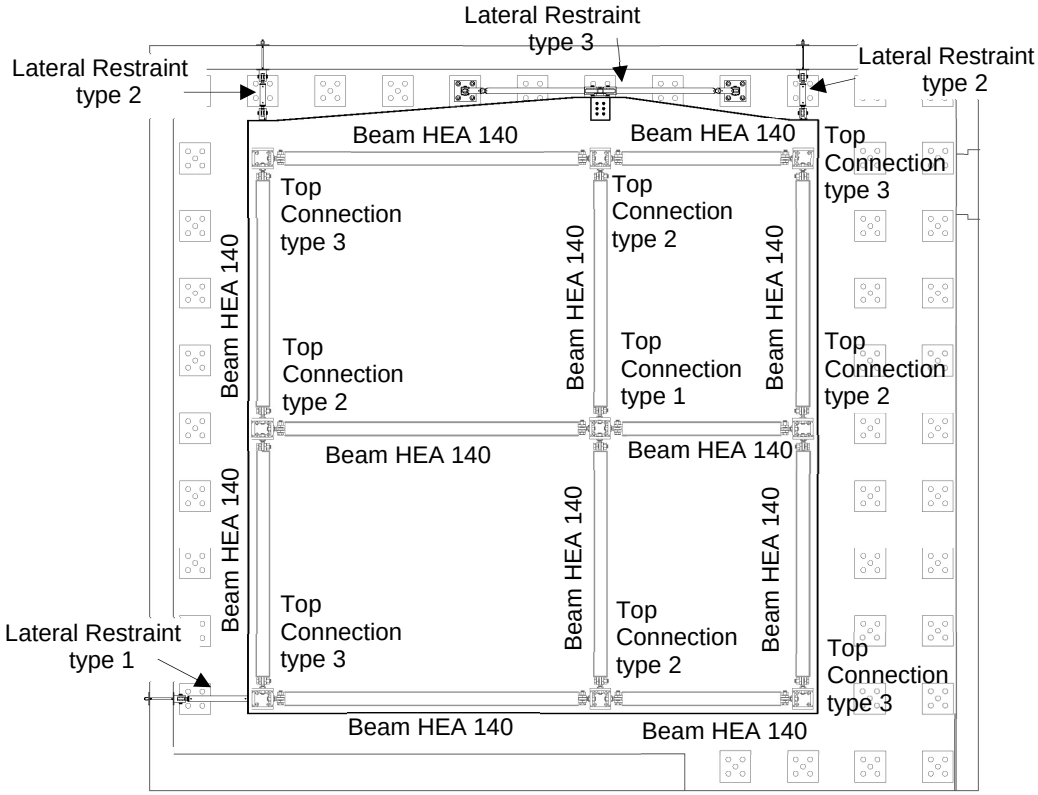

Figure 4-5. Restraints for the asymmetric full-scale specimen

4.3 Rebars

The reinforcement of the slabs of the two full-scale specimens is realized with an electrowelded wire mesh located on both the upper and the lower sides of the slab and additional rebars added where required by the design calculations.

A summary of the reinforcement needed for the slabs of the two full-scale specimens is reported in Table 4-3-Table 4-7. In detail:

- Table 4-3 summarises the electrowelded wire mesh required for both the specimens;
- Table 4-4 and Table 4-5 list the additional rebars for the symmetric specimen, for the lower and the upper side, respectively;
- Table 4-6 and Table 4-7 collect the additional rebars for the asymmetric specimen, related to the lower and the upper side, respectively.

A detailed description of the layout of the rebars for both the specimens is presented in Annex C.

Table 4-3-Table 4-7 and the drawings of Annex C have been sent to a local Company for their production.

Table 4-3. Summary of the electrowelded wires for the full-scale specimens (symmetric and asymmetric configuration)

ELECTROWELDED WIRES

MESH TYPE 1

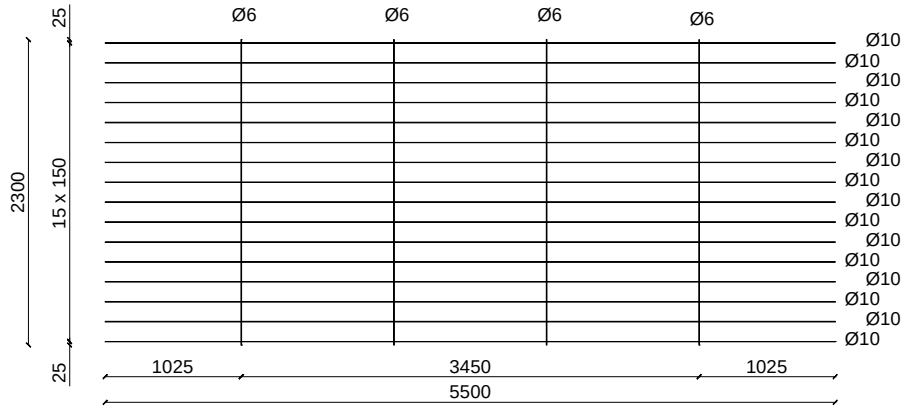

N° panels	Dimensions mm	Nominal unitary weight kgf	Nominal total weight kgf
22	5500x2300	57,882	1273

MESH TYPE 2

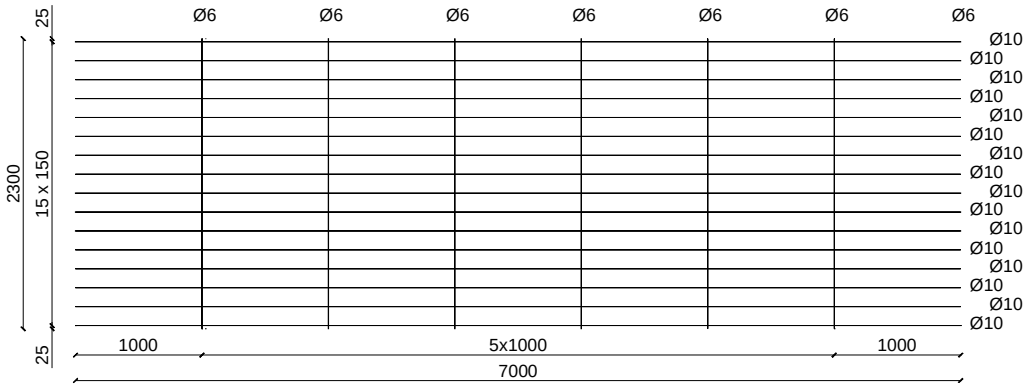

N° panels	Dimensions mm	Nominal unitary weight kgf	Nominal total weight kgf
62	7000x2300	74,493	4619

MESH TYPE 3

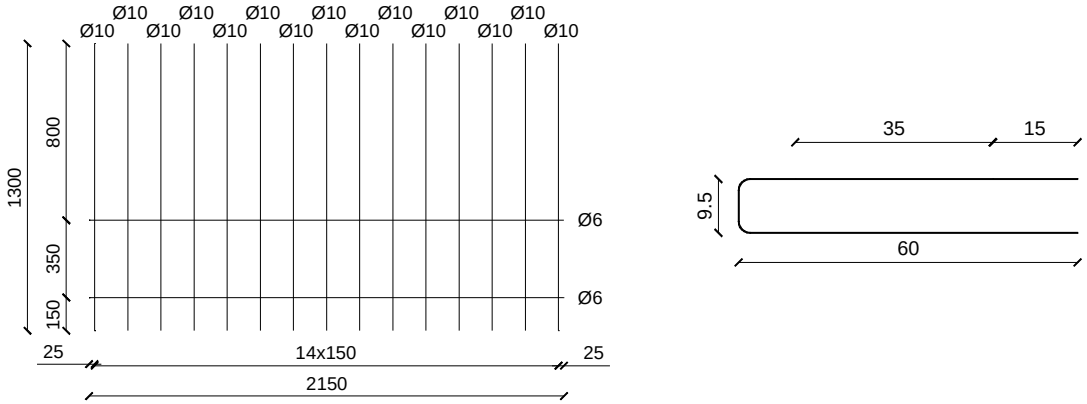

N° panels	Dimensions mm	Nominal unitary weight kgf	Nominal total weight kgf
44	2150x1300	12,976	571

Table 4-4. Summary of the rebars for the symmetric configuration - Lower side

SLAB REBARS - LOWER SIDE - SYMMETRIC CONFIGURATION					
Position	Shape	Diameter mm	Length mm	Quantity n°	Nominal weight kgf
Pos. C	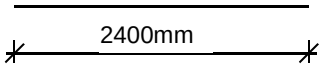	10	2400	22	33
Pos. D		10	2400	8	12
Pos. E	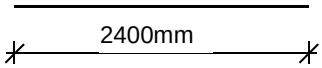	10	2400	30	44
Pos. F		10	2400	8	12
Total nominal weight (kgf)					153

Table 4-5. Summary of the rebars for the symmetric configuration - Upper side.

SLAB REBARS - UPPER SIDE - SYMMETRIC CONFIGURATION					
Position	Shape	Diameter mm	Length mm	Quantity n°	Nominal kgf
Pos. A	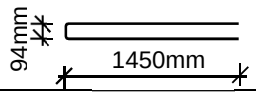	10	3000	28	52
Pos. G1	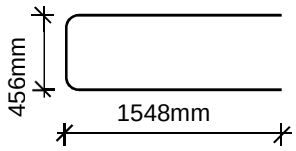	16	3500	3	17
Pos. G2	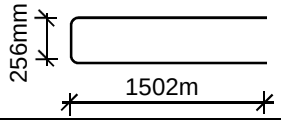	16	3200	3	15
Pos. H	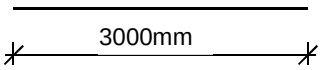	16	3000	24	114
Pos. I	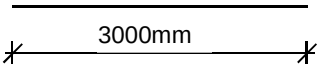	16	3000	48	227
Pos. L	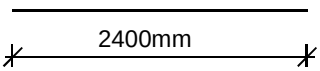	10	2400	92	136
Pos. M		16	3000	12	57
Pos. N		16	3000	44	206
Pos. O	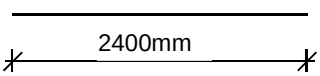	10	2400	35	52
Total nominal weight (kgf)					878

Table 4-6. Summary of the rebars for the asymmetric configuration - Lower side

SLAB REBARS - LOWER SIDE - ASYMMETRIC CONFIGURATION					
Position	Shape	Diameter mm	Length mm	Quantity n°	Nominal weight kgf
Pos. C	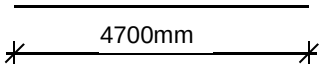	10	4700	41	119
Pos. D	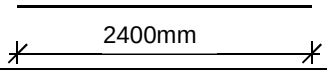	10	2400	8	12
Pos. E	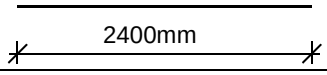	10	2400	21	31
Pos. F	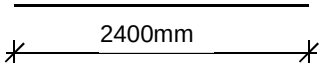	10	2400	8	12
Pos. G	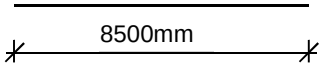	10	8500	8	42
Pos. H	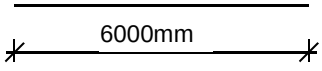	10	6000	76	281
Total nominal weight (kgf)					527

Table 4-7. Summary of the rebars for the asymmetric configuration - Upper side

SLAB REBARS - UPPER SIDE - ASYMMETRIC CONFIGURATION					
Position	Shape	Diameter mm	Length mm	Quantity n°	Nominal kgf
Pos. A	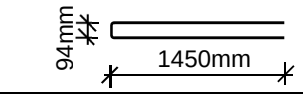	10	3000	28	52
Pos. I	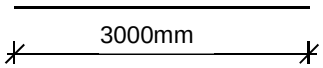	16	3000	40	189
Pos. L	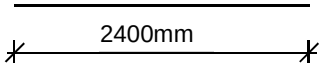	10	2400	98	145
Pos. M	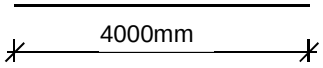	16	4000	12	76
Pos. N	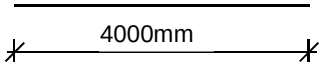	16	4000	45	284
Pos. O	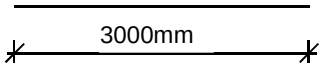	10	3000	35	65
Pos. P1	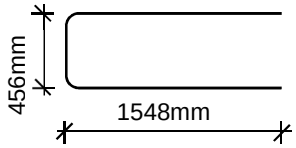	16	3500	3	17
Pos. G2	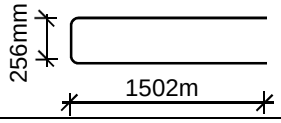	16	3200	3	15
Pos. Q	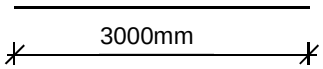	16	3000	24	114
Total nominal weight (kgf)					957

5 CONCLUDING REMARKS

This document focuses on the design work related to two full scale tests carried out at the University of Trento in the framework of the European RFCS project 'Robust Impact design of steel and composite building structures' (acronym ROBUSTIMPACT) (Grant Agreement Number: RFSR-CT-2012-00029).

The study focuses on composite steel and concrete framed buildings and in particular on their response when subject to accidental actions. At this aim, two reference five-story buildings were designed according to the Eurocodes, and representative one story sub-frames 'extracted' from them. The sub-frames were built and tested at the Laboratory of Material and Structural Testing (LMST) of the University of Trento by simulating the loss of an internal column. In this document, the work performed to design the reference frames, to 'extract' representative sub-frames, and to design the test set-up is highlighted. In detail, the following subjects are analyzed:

- the selection and the definition of the reference buildings for the case studies;
- the design of the reference buildings according to the Eurocodes;
- the identification of the representative sub-structures (slab-beam system, columns and joints) from the reference structures to be experimentally investigated;
- the design of the test set-up.

6 ACKNOWLEDGEMENTS

The experimental work presented in this document was supported by the European Commission under its Research Programme of the Research Fund for Coal and Steel (Project acronym Robust Impact, Grant Agreement Number: RFSR-CT-2012-00029) .

The Authors gratefully acknowledge prof. eng. Paolo Zanon, Mr. Stefano Girardi, Mr. Marco Graziadei and Mr. Alessandro Banterla for their valuable advices for the design of the experimental set-up.

7 LITERATURE

[1] CSI SAP 2000 – Linear and nonlinear static and dynamic analysis and design of three-dimensional structures: Basic analysis reference manual, Computers and Structures, Inc. Berkeley, California, 2011.
[2] EN 1993-1-8 – Eurocode 3: Design of steel structures - Part 1-8: Design of joints, EN 1993-1-8:2005, December 2010;
[3] EN 1992-1-1 – Eurocode 2: Design of concrete structures - Part 1-1: General rules and rules for buildings, CEN 2004.
[4] EN 1993-1-1 – Eurocode 3: Design of steel structures - Part 1-1: General rules and rules for buildings, CEN 2004.
[5] EN 1991-1-4 – Eurocode 1: Actions on Structures - Part 1-4: General actions - Wind Actions, CEN 2004.
[6] EN 1991-1-3 – Eurocode 1: Actions on Structures - Part 1-3: General actions - Snow Loads, CEN 2002.
[7] EN 1990 – Eurocode 0: Basis of Structural Design, CEN 2002.
[8] EN 1994-1-1 – Eurocode 4: Design of composite steel and concrete structures - Part 1-1: General rules and rules for buildings, CEN 2004.
[9] ABAQUS – Analysis user's manual, version 6.10, Simulia Dassault Systems, 2010.
[10] Allam SM, Shoukry MS, Rashad G, Hassan AS.. Evaluation of tension stiffening effect on the crack width calculation of flexural RC members. Alexandria Engineering Journal; 52: 163-173. 2013.
[11] Fu F, Lam D, Ye J. Modeling semi-rigid composite joints with precast hollowcore slabs in hogging moment region. Journal of Constructional Steel Research; 64(12): 1408-1419. 2008.